FAA-80-15, I

ADVANCED MICROSTRIP ANTENNA DEVELOPMENTS
Volume I - Technology Studies for Aircraft Phased Arrays

Gary G. Sanford
BALL AEROSPACE SYSTEMS DIVISION
Boulder CO   80306

JUNE 1981

FINAL REPORT

Prepared for

U.S. DEPARTMENT OF TRANSPORTATION
FEDERAL AVIATION ADMINISTRATION
Office of Systems Engineering Management
Washington DC   20591

1. Report No. FAA-EM-80-11	2. Government Accession No.	3. Recipient's Catalog No.
4. Title and Subtitle ADVANCED MICROSTRIP ANTENNA DEVELOPMENTS Volume I-Technology Studies for Aircraft Phased Arrays		5. Report Date June 1981
		6. Performing Organization Code
7. Author's) Gary G. Sanford		8. Performing Organization Report No. DOT-TSC-FAA-80-15, I
9. Performing Organization Name and Address Ball Aerospace Systems Division* P.O. Box 1062 Boulder CO 80306		10. Work Unit No. (TRAIS) FA189/R1134
		11. Contract or Grant No. DOT-TSC-1397-1
12. Sponsoring Agency Name and Address U.S. Department of Transportation Federal Aviation Administration Office of Systems Engineering Management Washington DC 20591		13. Type of Report and Period Covered Final Report April 1979 – June 1980
		14. Sponsoring Agency Code

15. Supplementary Notes

*Under Contract To: U.S. Department of Transportation
Research and Special Programs Administration
Transportation Systems Center
Cambridge MA 02142

16. Abstract

Work has continued on improvement of microstrip phased-array antenna technology since the first microstrip phased-array was flight-tested during the FAA 1974-1975 ATS-6 test program. The present development has extended this earlier work in three areas: the microstrip radiating elements, the array configuration, and the control circuitry. The effort has been successful in developing important new phased-array techniques. These techniques were demonstrated with working hardware, but a complete array was not within the scope of the program.

Radiating elements with broad beamwidths were required to permit steering the array to angles near endfire. The most significant improvement was the development of a microstrip crossed-slot element.

Dual-band or broad-band elements were developed to permit operation in both the recieve and transmit bands. Several approaches were experimented with, the most promising of which was the use of stacked crossed-slot elements. This achieves broad beamwidth and dual-band operation in a compact device.

Static arrays for end-fire operation were investigated, and a 4x4 array demonstrated promise for this application. Several phase shifters were developed; the three-bit switched-line phase shifters gave excellent performance.

Volume II: DOT-TSC-FAA-80-15,II/FAA-EM-80-12, Microstrip GPS Antennas for General Aviation Aircraft, 44 pages, will be published, July 1981.

17. Key Words Microstrip Antennas Mocrostrip Phase Shifters Phased Arrays Aircraft Antennas Aircraft – Satellle Communications	18. Distribution Statement DOCUMENT IS AVAILABLE TO THE PUBLIC THROUGH THE NATIONAL TECHNICAL INFORMATION SERVICE, SPRINGFIELD, VIRGINIA 22161		
19. Security Classif. (of this report) Unclassified	20. Security Classif. (of this page) Unclassified	21. No. of Pages 76	22. Price

Form DOT F 1700.7 (8-72)   Reproduction of completed page authorized

PREFACE

Under a previous contract with the U.S. Department of Transportation, Transportation Systems Center (DOT/TSC), Ball Brothers Research Corporation (now Ball Aerospace Systems Division) designed and built a conformal microstrip phased-array antenna which was installed on a KC-135 test aircraft and successfully operated with the NASA ATS-6 satellite during the 1974-1975 ATS-6 test program. This program and the phased-array antenna development were sponsored by the Federal Aviation Administration. In accordance with the requirements of the test program, the antenna developed was a linear array with limited scan capability which operated only in the satellite-aircraft receive band.

Since that time, work has continued on the development of advanced microstrip antenna technology for aircraft-satellite communications. The earlier work has been extended in three areas: broad-band, broad-beamwidth microstrip radiators; array configurations; and phase shifters. A complete array suitable for aircraft use was not within the program scope; however individual components and bread board arrays were built and tested.

The work was directed by the TSC Project Engineer, Leslie Klein.

METRIC CONVERSION FACTORS

Approximate Conversions to Metric Measures

Symbol	When You Know	Multiply by	To Find	Symbol
		LENGTH		
in	inches	2.5	centimeters	cm
ft	feet	30	centimeters	cm
yd	yards	0.9	meters	m
mi	miles	1.6	kilometers	km
		AREA		
in²	square inches	6.5	square centimeters	cm²
ft²	square feet	0.09	square meters	m²
yd²	square yards	0.8	square meters	m²
mi²	square miles	2.6	square kilometers	km²
	acres	0.4	hectares	ha
		MASS (weight)		
oz	ounces	28	grams	g
lb	pounds	0.45	kilograms	kg
	short tons (2000 lb)	0.9	tonnes	t
		VOLUME		
tsp	teaspoons	5	milliliters	ml
Tbsp	tablespoons	15	milliliters	ml
fl oz	fluid ounces	30	milliliters	ml
c	cups	0.24	liters	l
pt	pints	0.47	liters	l
qt	quarts	0.95	liters	l
gal	gallons	3.8	liters	l
ft³	cubic feet	0.03	cubic meters	m³
yd³	cubic yards	0.76	cubic meters	m³
		TEMPERATURE (exact)		
°F	Fahrenheit temperature	5/9 (after subtracting 32)	Celsius temperature	°C

Approximate Conversions from Metric Measures

Symbol	When You Know	Multiply by	To Find	Symbol
		LENGTH		
mm	millimeters	0.04	inches	in
cm	centimeters	0.4	inches	in
m	meters	3.3	feet	ft
m	meters	1.1	yards	yd
km	kilometers	0.6	miles	mi
		AREA		
cm²	square centimeters	0.16	square inches	in²
m²	square meters	1.2	square yards	yd²
km²	square kilometers	0.4	square miles	mi²
ha	hectares (10,000 m²)	2.5	acres	
		MASS (weight)		
g	grams	0.035	ounces	oz
kg	kilograms	2.2	pounds	lb
t	tonnes (1000 kg)	1.1	short tons	
		VOLUME		
ml	milliliters	0.03	fluid ounces	fl oz
l	liters	2.1	pints	pt
l	liters	1.06	quarts	qt
l	liters	0.26	gallons	gal
m³	cubic meters	35	cubic feet	ft³
m³	cubic meters	1.3	cubic yards	yd³
		TEMPERATURE (exact)		
°C	Celsius temperature	9/5 (then add 32)	Fahrenheit temperature	°F

°F   -40   0   32   80   98.6   120   160   200   212

°C   -40   -20   0   20   37   40   60   80   100

TABLE OF CONTENTS

LIST OF TABLES

LIST OF ILLUSTRATIONS

LIST OF ILLUSTRATIONS (Continued)

LIST OF ILLUSTRATIONS (Continued)

1. SUMMARY AND CONCLUSIONS

During the 1974-1975 ATS-6 test program a conformal microstrip phased-array antenna was successfully designed, fabricated and tested, and then flown on an FAA KC-135 test aircraft. The present development has extended this previous work in three areas: the microstrip radiating elements, the array configuration, and the control circuitry. The effort has been successful in developing significant new phased array techniques. These techniques were demonstrated with working hardware, but a complete array was not within the scope of the program.

Radiating elements with broad beamwidths were required to permit steering the array to angles near end fire. The first improvement was to etch a standard microstrip element on a high-dielectric-constant substrate so that the aperture area could be reduced. The most significant improvement was the development of a microstrip crossed-slot.

Dual-band or broad-band elements were required to permit operation in both the receive and transmit bands. The best solution to this problem was to use two elements, stacked one on top of the other, each resonant at one of the desired frequencies. A resonant matching circuit on a single element was also successful, but there was some doubt whether it could be reproduced with normal production tolerances. Finally, a simple broad-band approach using a thick element resembling a conventional cavity-backed radiator was demonstrated, but all the models using this approach had a gain roll-off of at least 1 dB at the frequencies of interest.

Static arrays on 2x8 and 4x4 matrices were fabricated and tested. A 4x4 array of crossed slots was found to be the superior configuration. Array degradation due to typical phase and amplitude errors was investigated analytically and found to be negligible. Brief consideration was given to a switched array.

Phase-shifter development was initially concentrated on the quadrature-hybrid shifter. However, when constant phase-versus-frequency was found unnecessary and when series-diode power handling was demonstrated, the switched-line phase-shifter was preferred. A three-bit switched-line phase-shifter was designed and demonstrated.

As a result of this program, techniques have been developed that overcome most of the limitations of the original phased-array. The development of the full array satisfying the extended requirements discussed earlier can now be pursued with minimum risk.

2   INTRODUCTION

The characteristics of future satellite systems for oceanic aeronautical communications has been the subject of considerable study. It is widely recognized that the availability of a practical antenna with gain in excess of 10 dB would add to the range of alternatives available to system designers. The work presented here is an attempt to use the potential of low fabrication costs and ease of installation, which are characteristics of microstrip, to develop phased-array components and prototype arrays which meet the gain requirements and other antenna design goals. The developments presented here are part of an effort to extend the antenna design activities carried out in 1974-1975 as part of the U.S. Department of Transportation's participation in the international ATS-6 satellite test program.

Under contract with the U.S. Department of Transportation, Transportation Systems Center, Ball Brothers Research Corporation (now Ball Aerospace Systems Division) designed and built a conformal microstrip phased-array antenna which was installed on an FAA KC-135 test aircraft and successfully operated during the 1974-1975 ATS-6 test program. The antenna developed and tested at that time was an eight-element linear array of circularly polarized microstrip radiators operating in the satellite-aircraft receive band (1543.5-1558.5 MHz). The array, circumferentially mounted on the aircraft fuselage, produced a fan-beam pattern electronically steerable in elevation with beam steering effected by three-bit digital phase-shifters.

The present development has extended this previous work in three areas: the microstrip radiating elements, the array configuration, and the control circuitry. This effort has been directed toward the development of new techniques: array breadboards have been built in order to experiment with promising configurations, but the development of a complete array is left as a later task.
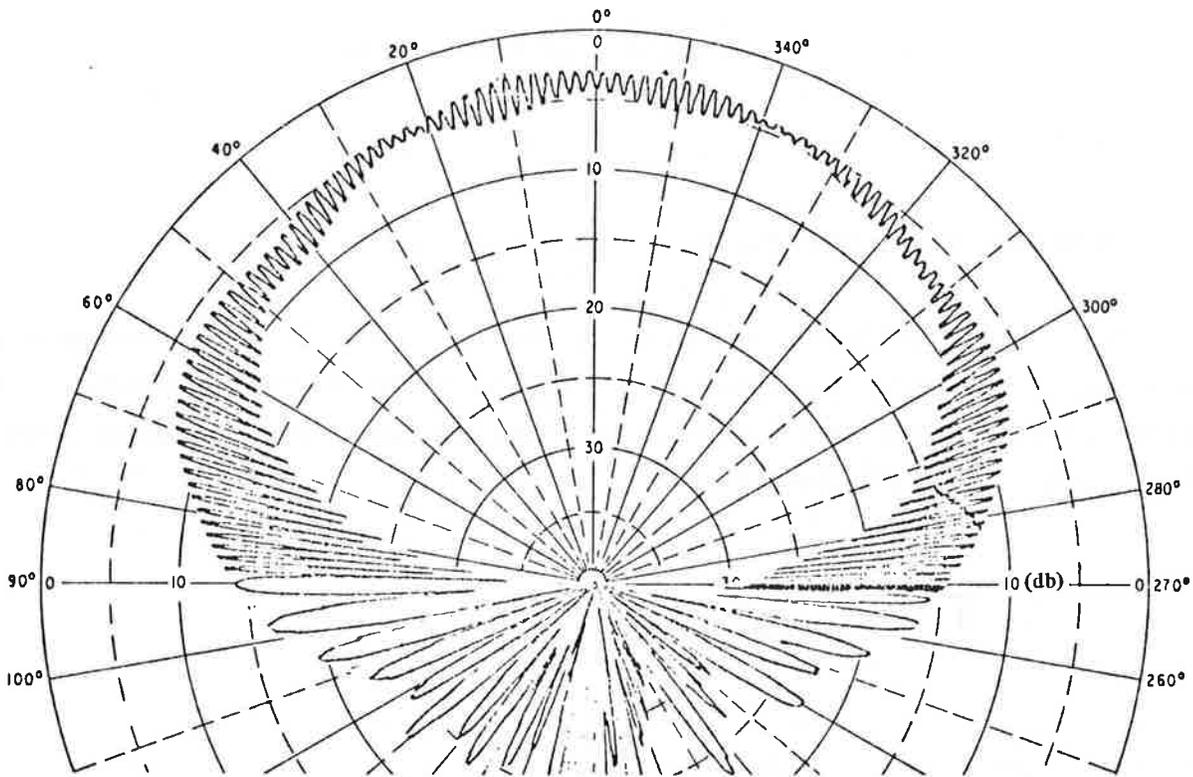
Rotating Linear Polarization
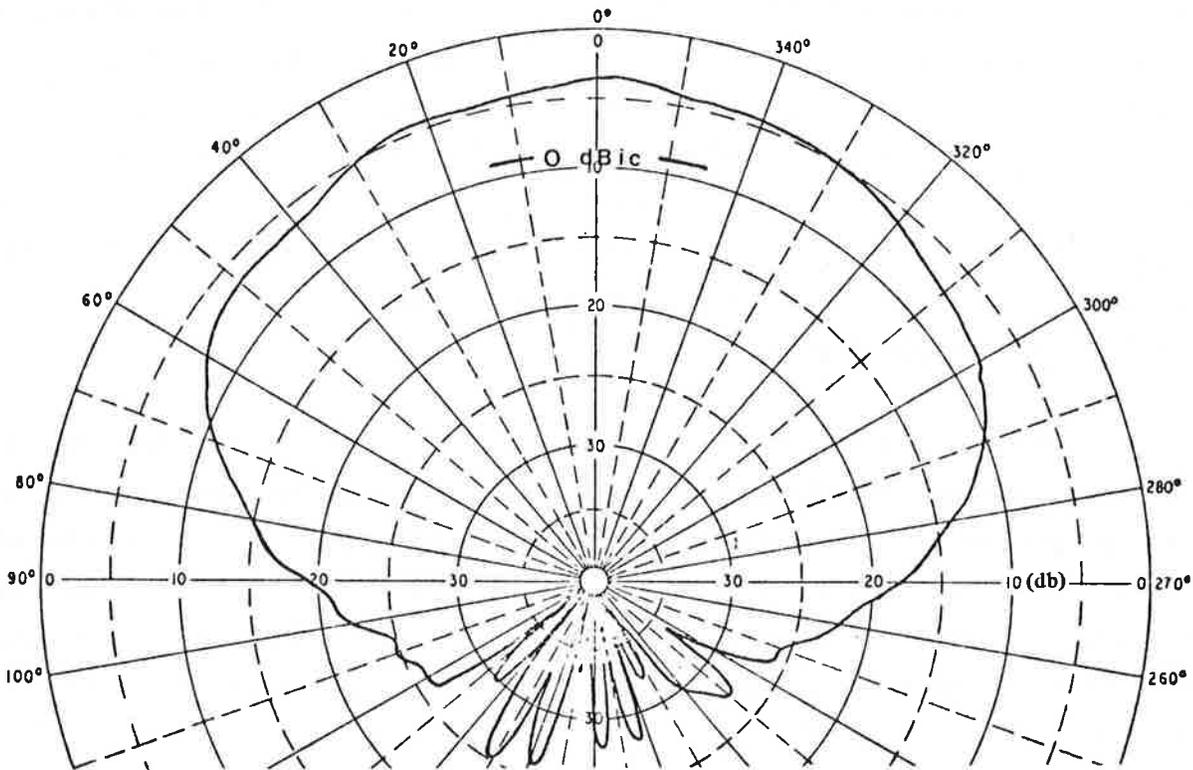
Circular Polarization

Figure 3-1 Radiation Patterns of a Standard Circularly Polarized Microstrip Element

3-2
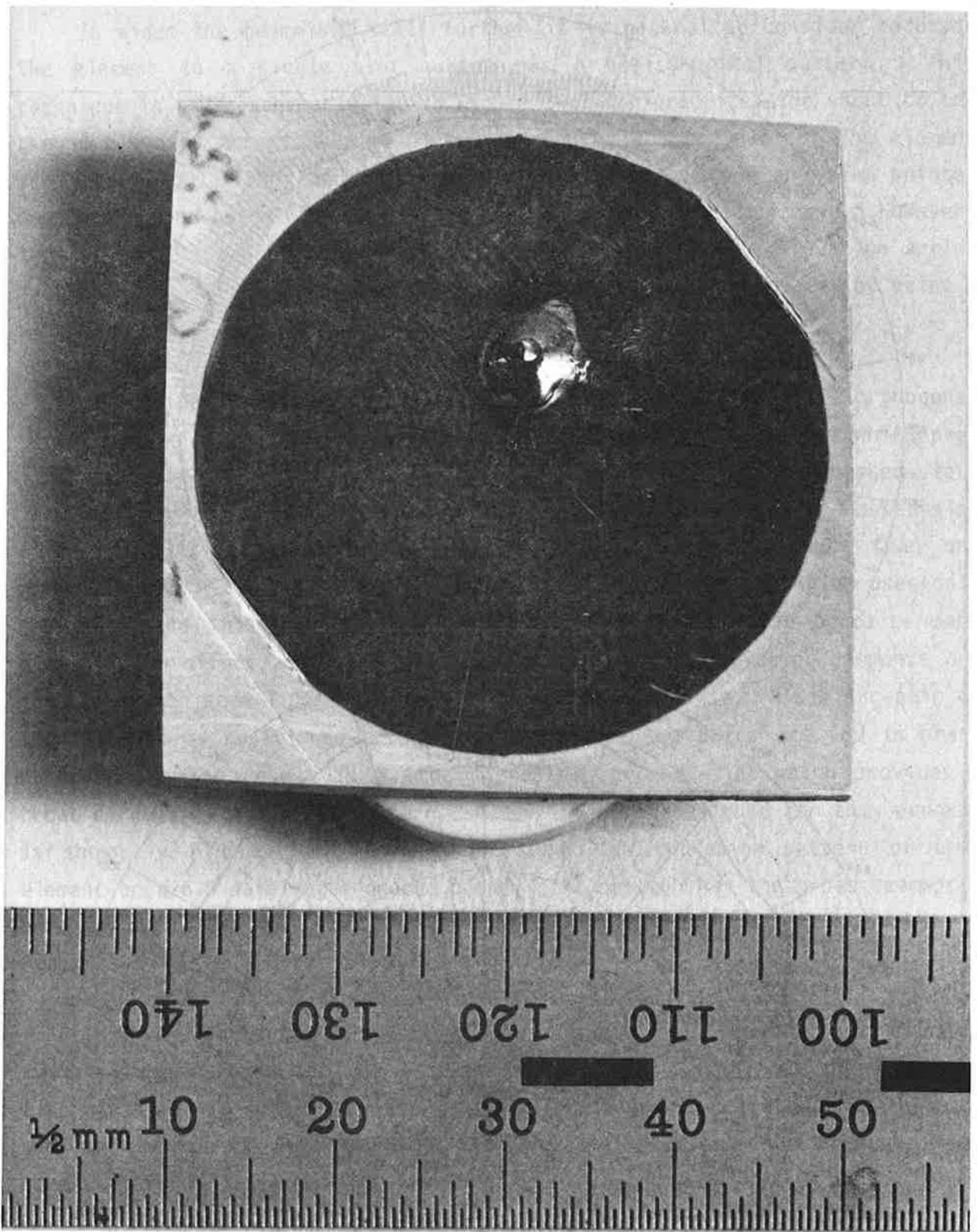
Figure 3-2   Photograph of a Microstrip Element Fabricated on a High-Dielectric-
Constant Substrate

FEED

RADIATING SLOT

SHORT TO GROUND PLANE

GROUND PLANE
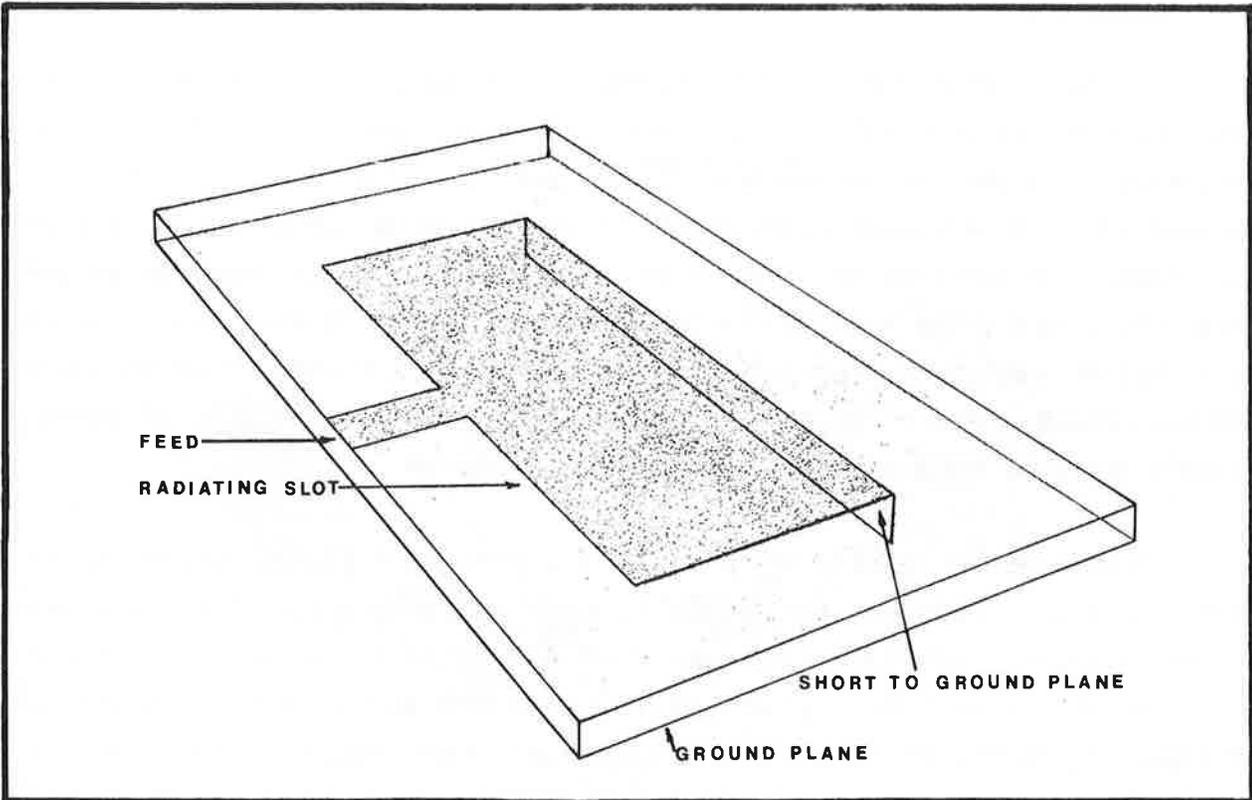
Figure 3-4 Quarter-Wave Resonant Microstrip Element

0°

90°

270°

180°
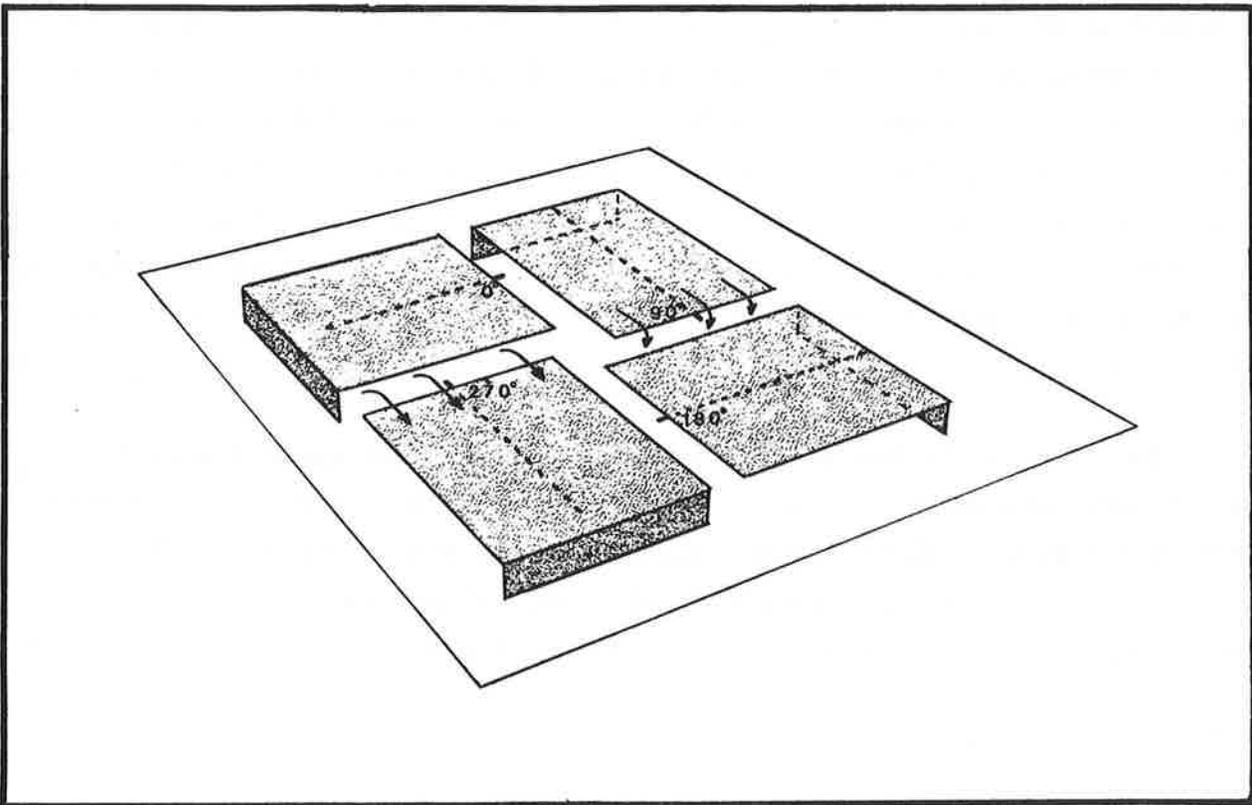
Figure 3-5 Concept for a Microstrip Crossed-Slot Radiating Element
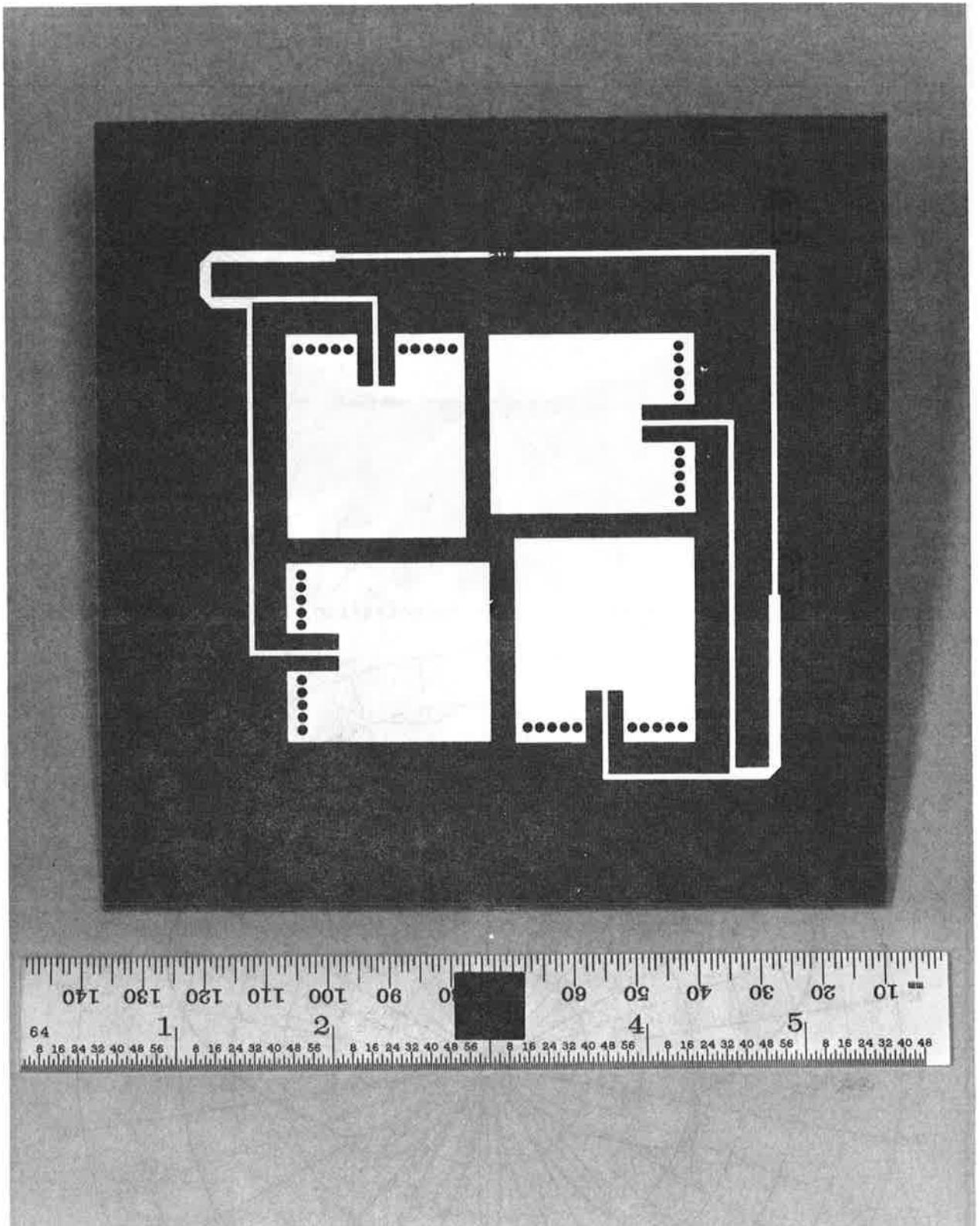
Figure 3-6 Working Model of Microstrip Crossed-Slot Element

Rotating Linear Polarization

Circular Polarization
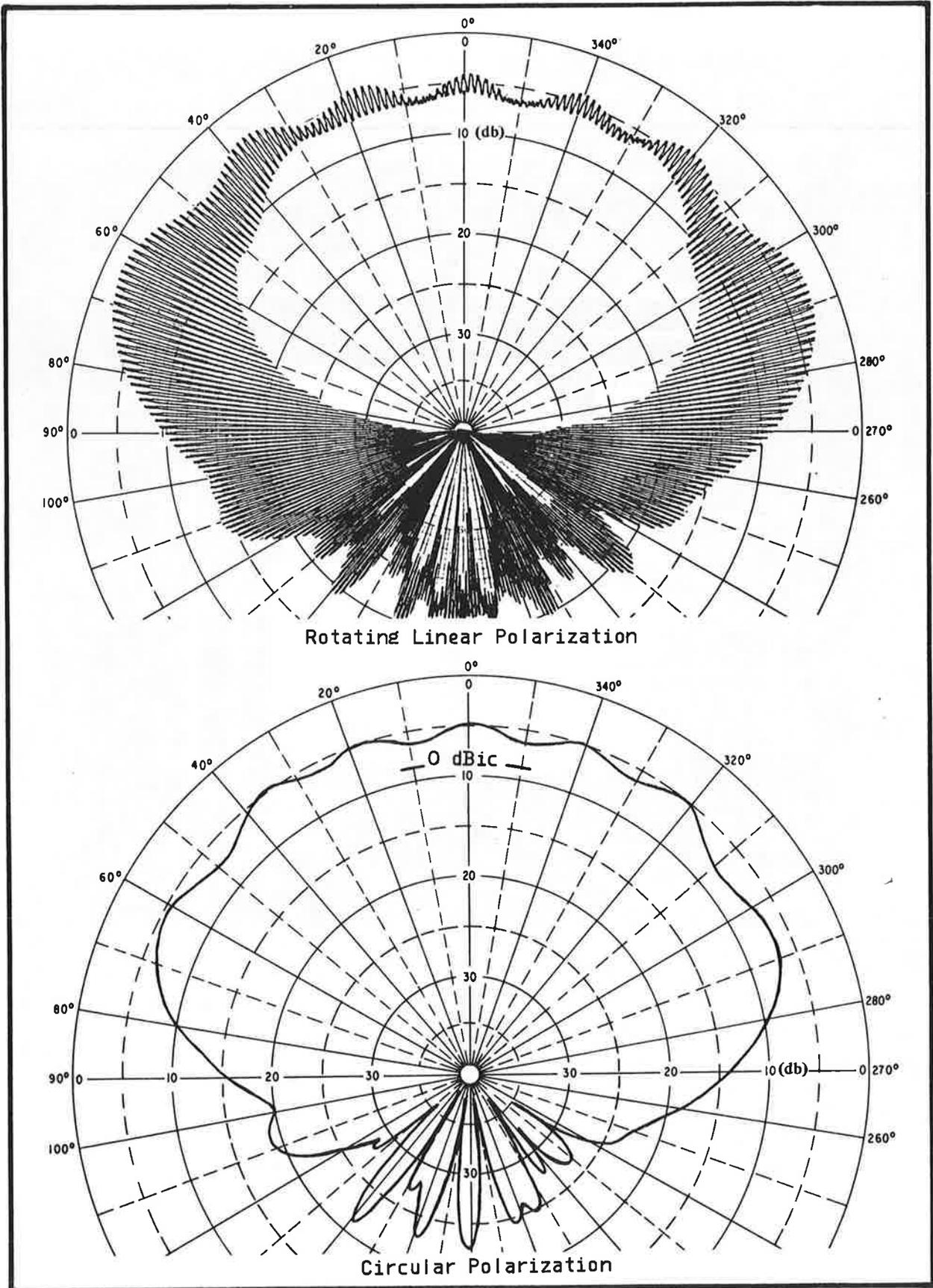
Figure 3-7 Radiation Patterns of a Microstrip Crossed-Slot Element

3-8

The crossed-slot sub-element as shown in Figure 3-5 is typically fed at a point along the dashed line. However, a more compact feed network can be achieved by feeding the sub-element at a corner near the center of the total element. The resulting asymmetry causes the sub-elements to couple with each other, and makes the matching effort more difficult. The solution to this problem was to make the sub-elements symmetrical about the element diagonals as shown in Figure 3-8.

When the elements are combined in an array, the copper laminate in which the slots are etched must be continuous beyond the bounds of the element. This will provide both a ground plane for the array feed network and a surface in which to etch the other elements of the array. The element shown in Figure 3-8 does not provide the continuous copper surface and must be modified as shown in Figure 3-9. The method used to feed the configurations of Figures 3-8 and 3-9 would depend on the application and is not shown. This configuration is recommended for the final array regardless of whether the element is stacked dual-band, stub-tuned dual-band, or broad-band. The modification does not change the pattern or basic impedance of the crossed-slot element.
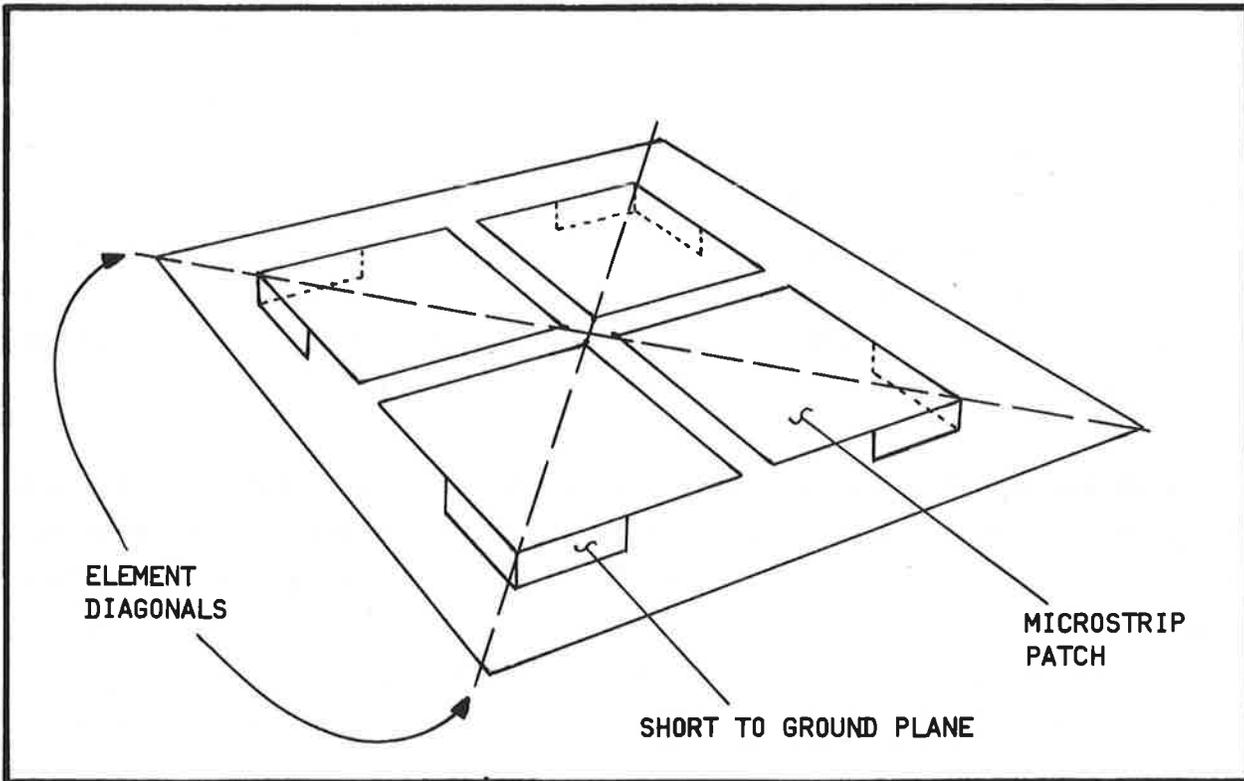
Figure 3-8 Microstrip Crossed Slot with Symmetrically Shorted Edges
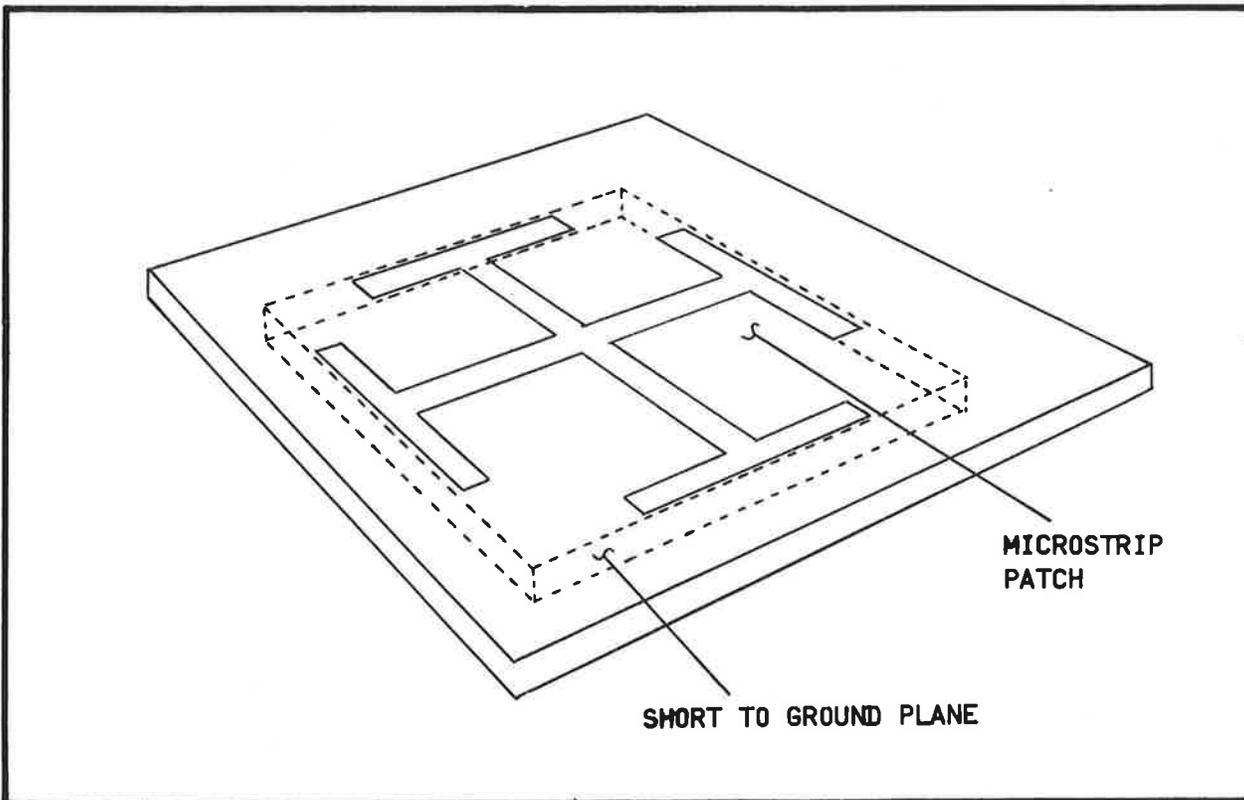
Figure 3-9   Microstrip Crossed Slot with Extended Upper Ground Plane, Continuously
Shorted Around the Perimeter

4   ELEMENT WITH RECEIVE AND TRANSMIT CAPABILITY

4.1   INTRODUCTION

Since a typical microstrip element has a bandwidth of about 2%, it is not naturally suited for receive and transmit bands separated by more than 7%, a requirement dictated by the satellite-mobile frequency allocations. However, during this program, three techniques were developed to overcome the bandwidth limitation.

4.2   STACKED DUAL-FREQUENCY ELEMENT

The best dual-frequency element for most array applications was found to be a stacked element. Physically, this antenna differs from other microstrip radiators by the introduction of an additional element or elements between the primary microstrip radiator and its associated ground plane. In Figure 4-1 the elements for the two-frequency case are shown as rectangular half-wave resonant patches, but they could be any form of microstrip radiator, including a crossed slot. The imbedded elements are simply laid out the same as the top element and scaled to the appropriate frequencies. The largest element is always nearest the ground plane with the smaller element or elements stacked in the order of their resonant frequencies. With this arrangement, the smallest element will always be the driven element.

The operation of the stacked element is understood by means of the equivalent circuit sketched in Figures 4-2 and 4-3. The sketches show a typical half-wave-resonant element in cross section. The elements are effectively connected in series through the fields that exist between them. At the lower frequency Figure 4-2 is applicable. Element A is below its resonance so that it is coupled to element B with a small inductive reactance. This coupling provides the connection from the feed point to element B. Radiating fields are excited between element B and the ground plane C at the resonant frequency of element B. At the higher frequency, Figure 4-3, element B is above its

Figure 4-1 Concept for a Stacked Dual-Frequency Microstrip Element

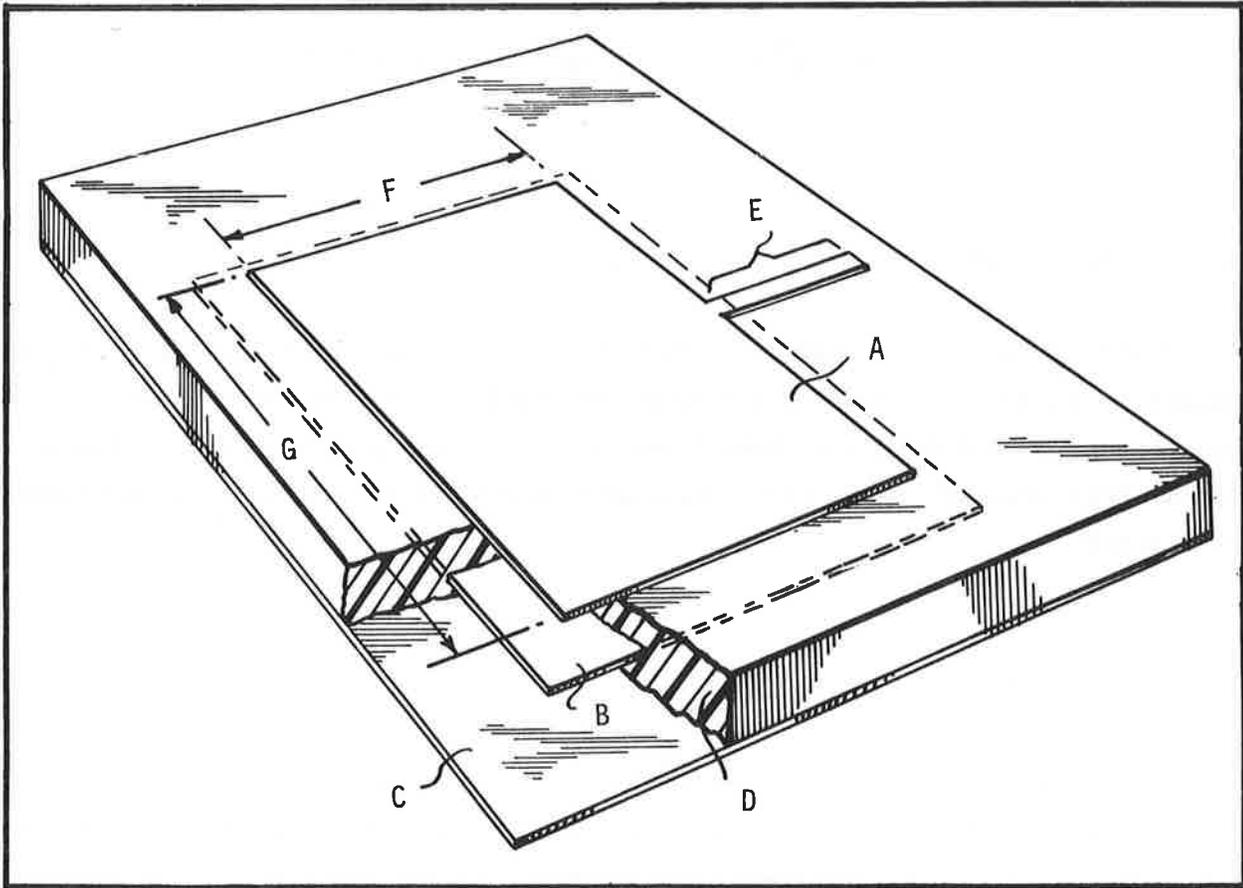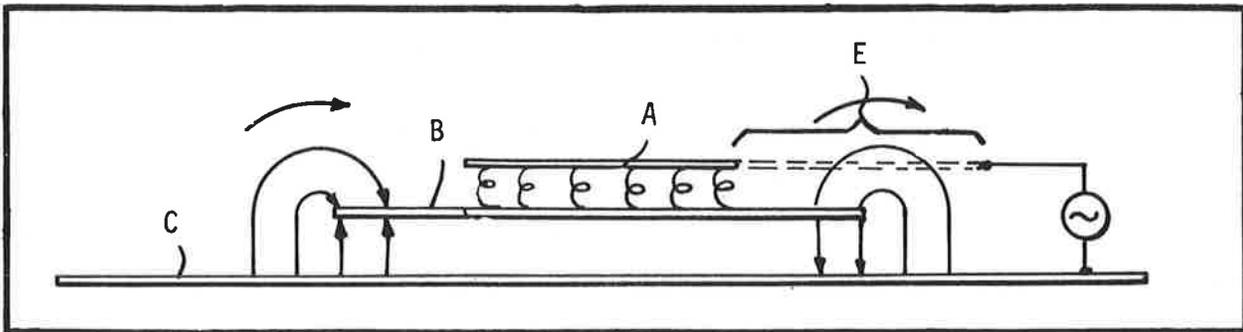Figure 4-2 Low-Frequency Equivalent Circuit for Stacked Microstrip Element
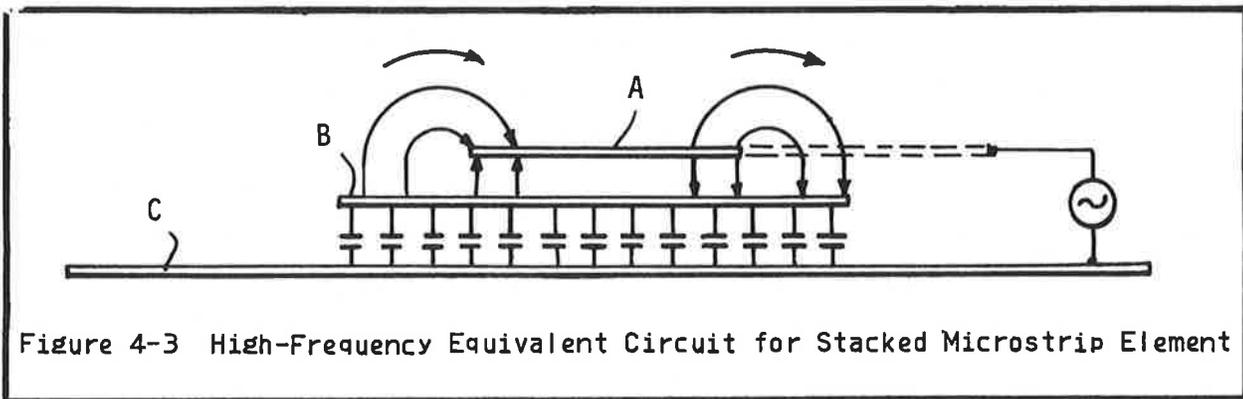
Figure 4-3 High-Frequency Equivalent Circuit for Stacked Microstrip Element

resonance so that it is capacitively coupled to the ground plane C. Now element B is effectively an extension of the ground plane, and radiating fields are excited between element A and element B at the resonant frequency of element A.

Since the reactance of one element must be very small at the resonance of the other, care must be taken to assure that the resonant bandwidth of one element does not extend into the bandwidth of the other element. If the substrates are thick so that bandwidths are large, then the resonances must be widely separated. If the bandwidth is reduced by using thinner substrates, then the two resonances can be closer together. An experiment was performed to determine just how thick the substrates could be in this application. Minimum frequency separations for three different thicknesses were found to be:

~ 50 MHz for .031" Teflon fiberglass
~ 70 MHz for .062" Teflon fiberglass
~ 120 MHz for .125" Teflon fiberglass

The .125" Teflon fiberglass is marginal for the intended frequency span, and therefore the .062" substrate was selected.

Figure 4-4 shows an elementary crossed-slot embodiment of this technique. This element performs quite satisfactorily, but the feed lines occupy space that in an array would have to be used by other components. To avoid this problem the feed lines may be located on a separate circuit board above the element as shown in an exploded view, Figure 4-5. Two variations of this top fed element are shown in Figures 4-6 and 4-7. Both of these elements perform well. The configuration of Figure 4-6 has the advantage of compactness which leaves more room for phase-shifter circuitry.

The configuration of Figures 4-7 and 4-8 has the advantage of easily re-alized transmission line widths and was the one recommended for use.

Figures 4-4 to 4-7 present condensed information on the techniques considered. Photographs of the elements are presented as well as a short descriptive paragraph and in the case of Figures 4-4, 4-5 and 4-7, a measured impedance plot is given as well.

4.3 RESONANT CIRCUIT FOR DUAL-FREQUENCY RESPONSE

Another approach to increasing the bandwidth of the microstrip element is to add a resonant circuit to the radiating element. This can be designed to provide an impedance match at two distinct frequencies, specifically, the required receive and transmit frequencies. To illustrate this technique, Figure 4-9 shows the impedance plot of a typical microstrip element, Plot A. Plot B shows the impedance of a series resonant circuit which can be added to the element impedance to achieve Plot C. An easy way to implement the series resonant circuit is to use two stubs with admittances shown in Figure 4-10, Plots D and E. When the two stubs are connected in parallel, the added admittances yield Plot F. When a quarter wavelength of transmission line is connected in front of this circuit, the admittance rotates half-way around the Smith Chart so that Plot F now represents the impedance of the circuit. This is the desired series resonant impedance, Plot B in Figure 4-9. A schematic of the resulting circuit is shown in Figure 4-11a. An antenna using this technique is shown in the Figure 4-12.

An important variation of this technique is explained using the same Smith Chart plots. A quarter wavelength of transmission line is connected to the element so that Plot A in Figure 4-9 now represents the element admittance. Plot B shows the admittance of a parallel resonant circuit which can be added to the element admittance to achieve Plot C. Using the same two stubs as before, a parallel resonance is achieved with an admittance shown in Plot F, Figure 4-10. No additional length of line is needed because this admittance is just that which is required in Plot B, Figure 4-9. Figure 4-11b shows a schematic of the second technique, and Figure 4-13 shows an antenna that uses this technique.
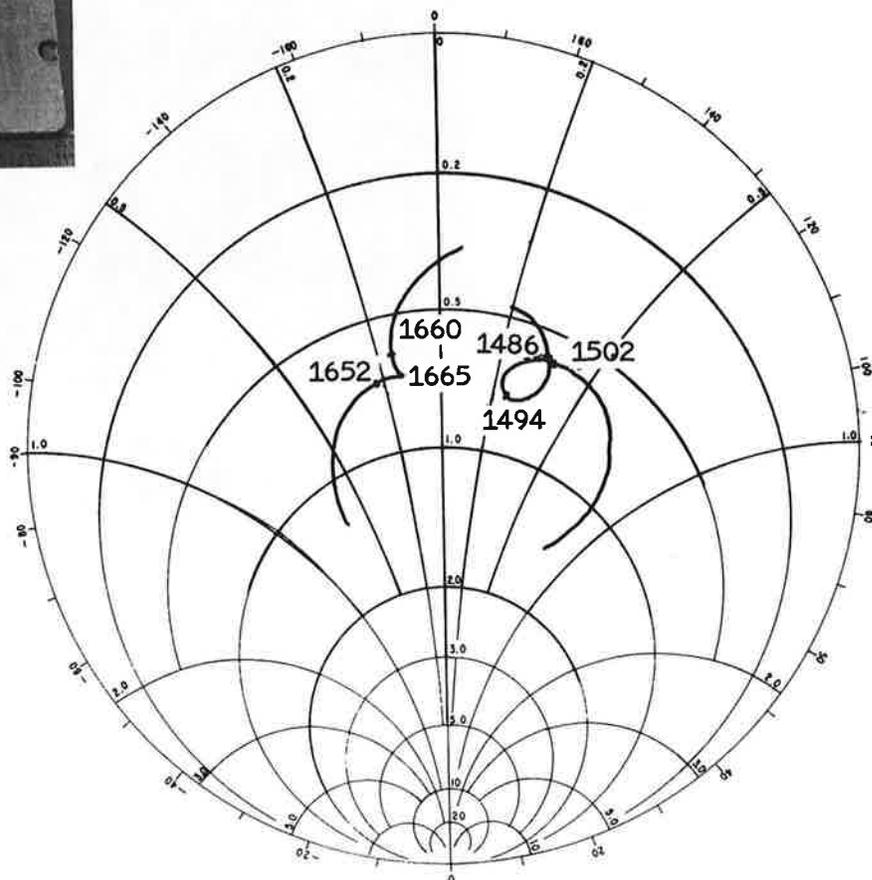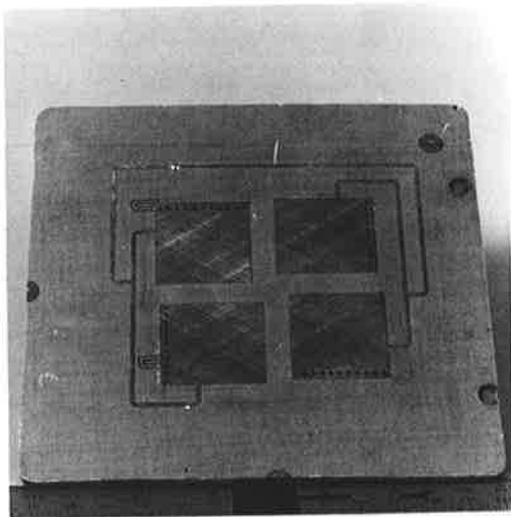
Figure 4-4 Stacked Dual-Frequency Microstrip Crossed Slot (Photograph and
            Impedance Plot)

The feed lines for this stacked dual-band element use the same ground plane
that the element uses. This takes up additional surface area, but has the
advantage of requiring only two laminated circuit boards. A convenient sub-
element impedance is obtained by feeding the sub-element on its side. The
impedance match is shown. Radiation patterns were identical with those of
the other crossed-slots. The gain was about 2 dB, indicating the possibil-
ity of feed-line losses. However, with little additional work, this element
would be useful in an application such as the Global Positioning System (GPS),
where near-hemispherical coverage at two frequencies is desired.
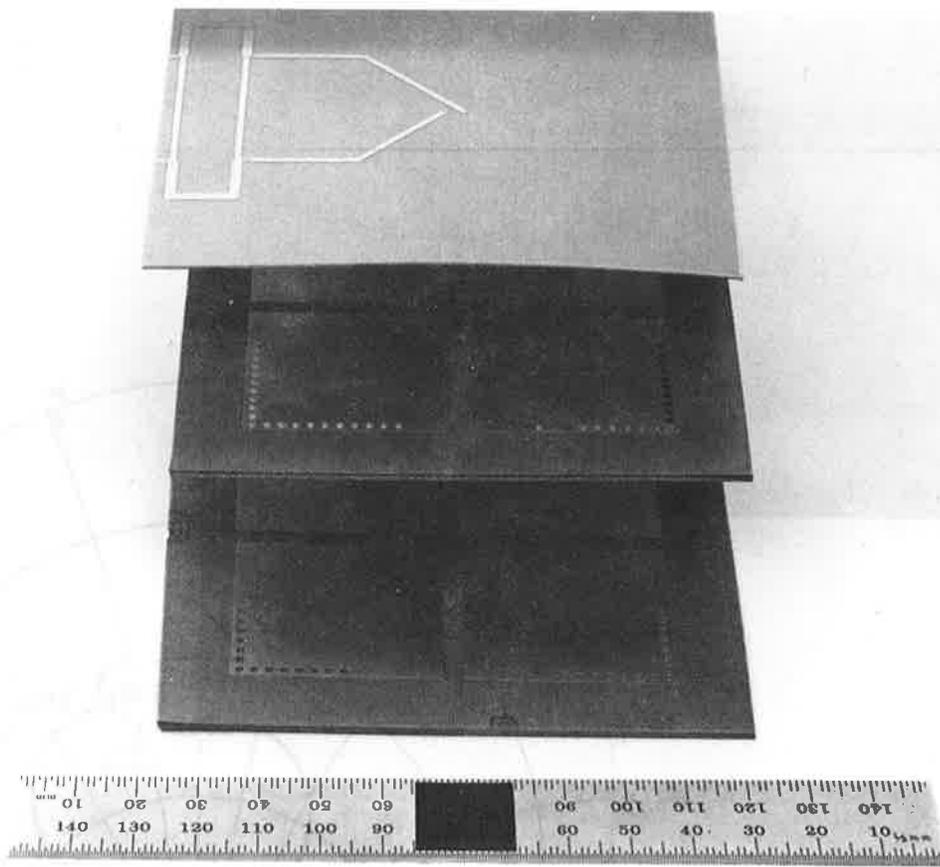
Figure 4-5 Exploded View, Stacked Microstrip Crossed Slot with Top Feed

This photograph reveals the essential features of the antenna. The ground plane for the feed lies on top of the upper element but is etched away in areas where it could interfere with the slots. The design assumes DC continuity between the upper and lower elements and the ground plane through the plated-through holes. The laminated structure does not easily allow this, thus the element was tested with and without a connection between the boards. The results were the same in either case. This greatly simplifies the fabrication of the array.

4-6
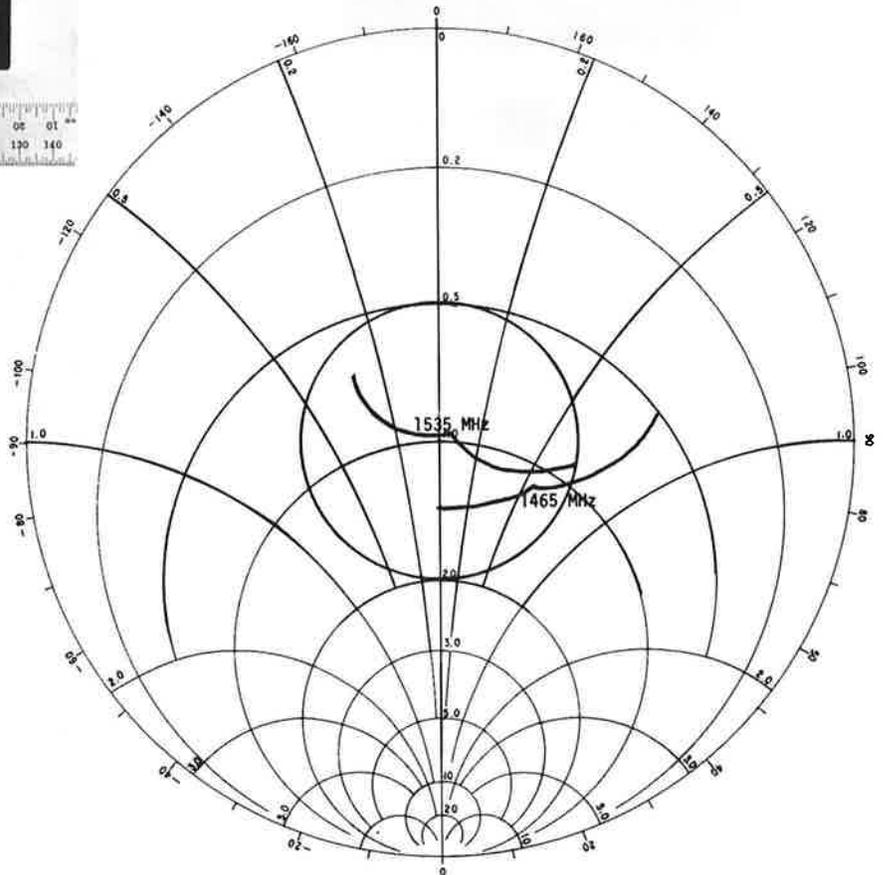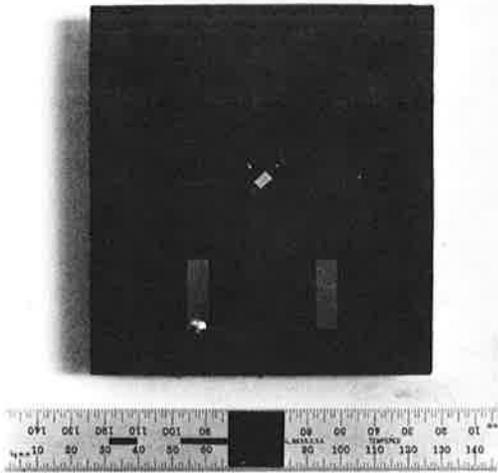
Figure 4-6 Top-Fed, Stacked Crossed-Slot Microstrip Antenna Photograph and
Impedance Plot, High-Impedance Feed

This element is essentially a laminated version of the exploded antenna shown
in Figure 4-5. Opposite pairs of sub-elements are driven in series from a
relatively high impedance point. The doubling of an already high impedance
produces an impedance that is difficult to match. The very narrow and very
wide lines in each feed are transformers necessary for achieving the desired
match. The resulting impedance separation plot shows that some correction
is necessary to achieve the desired frequency, but the antenna does perform
satisfactorily in two separate bands. The patterns were identical with those
of the other crossed-slot designs.

4-7
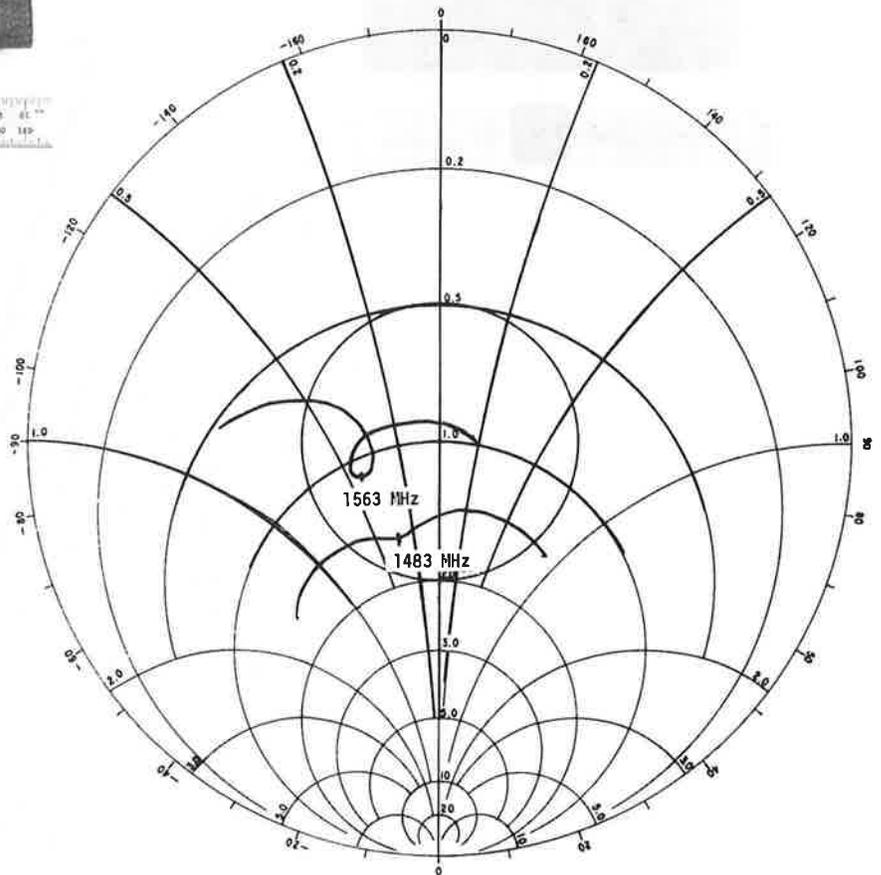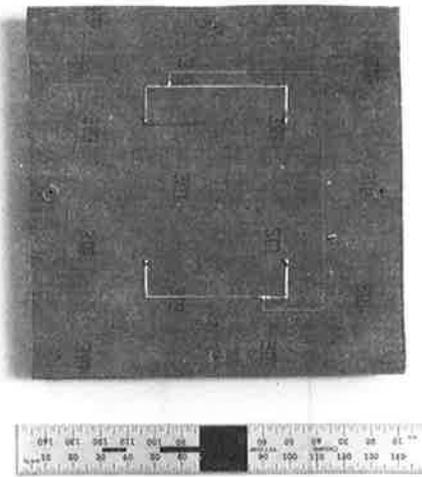
Figure 4-7 Top-Fed, Stacked Crossed-Slot Microstrip Antenna Photograph and
Impedance Plot, Low-Impedance Feed

In this preferred design, each sub-element is fed individually at a point where
the impedance is quite workable. To excite the sub-element at this lower
impedance point, the microstrip transmission line in this breadboard version is
connected to a wire passing through the sub-element and shorted to the element
ground plane. In practice the microstrip transmission line would be shorted to
the ground plane by a plated-through hole or eyelet. This was the most easily
implemented of all the dual frequency designs. The dual frequency response is
shown in the impedance plot. The patterns were identical to those of the other
crossed-slot designs.

4-8
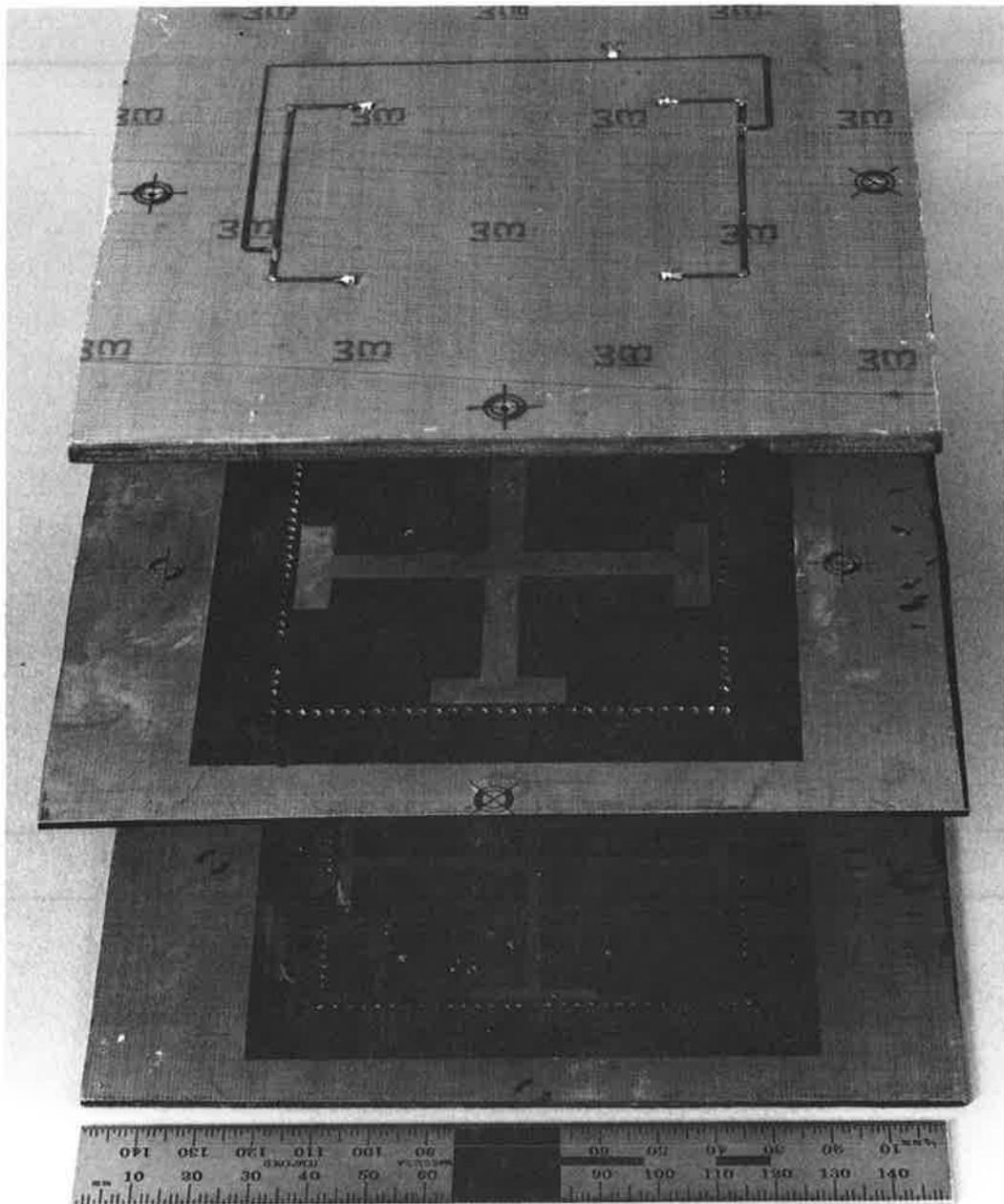
Figure 4-8 Exploded View of the Preferred Stacked Dual-Frequency Element

The various sub-elements making up the element are visible in this view. At
the top is the feed network, below it the high frequency sub-element and on
the bottom is the low frequency sub-element.
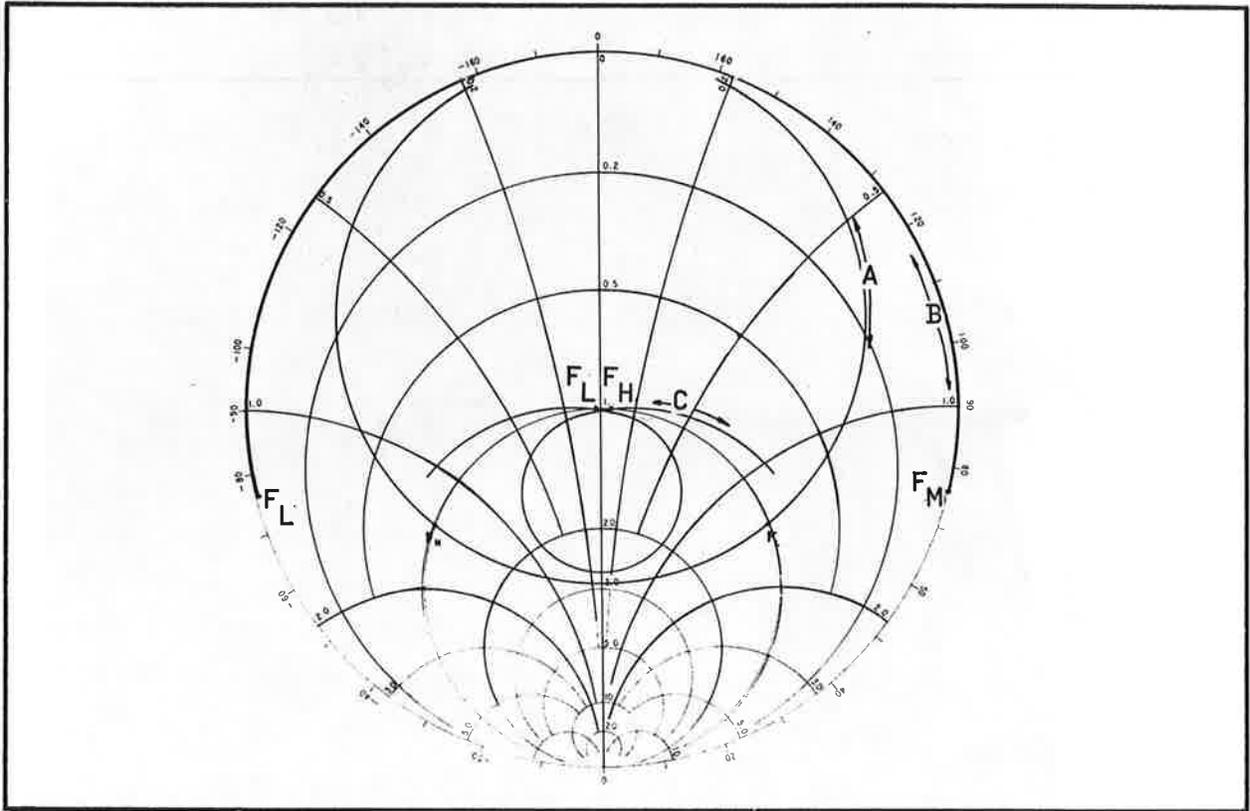
Figure 4-9 Dual-Band Match with Resonant Stubs
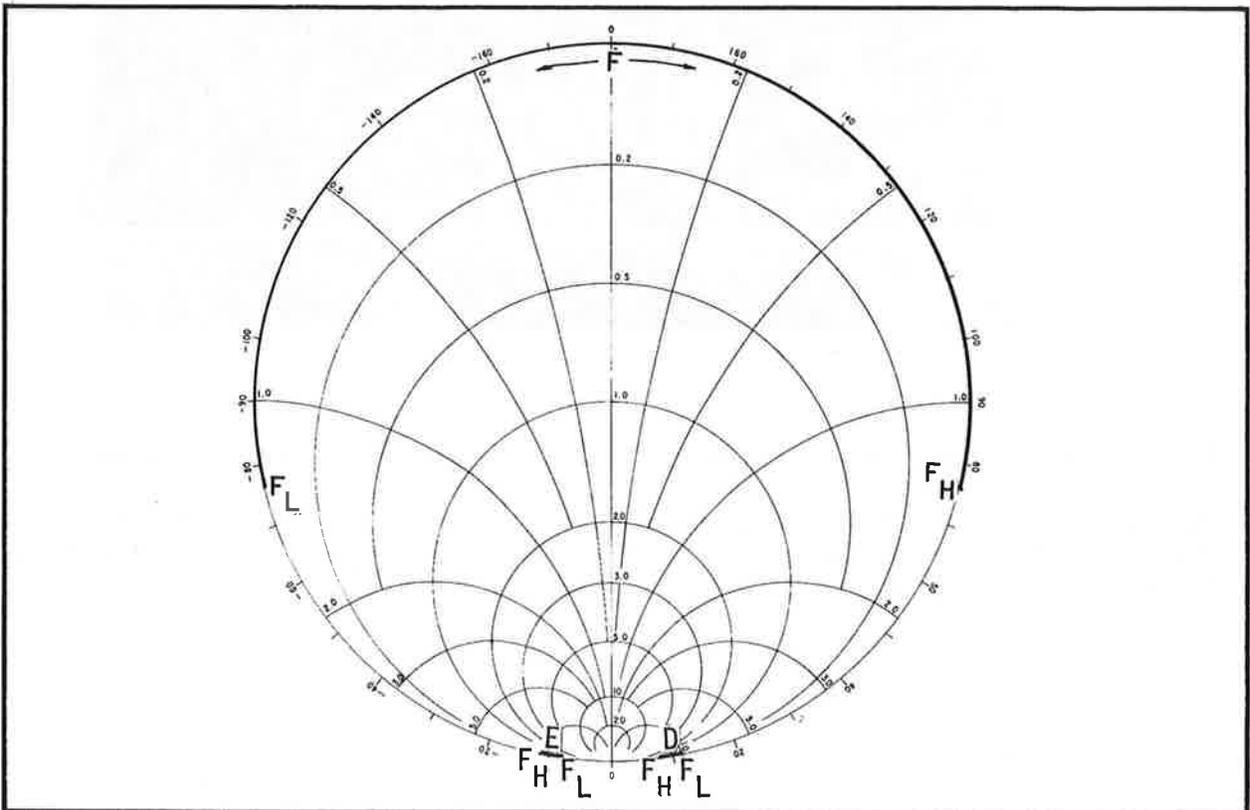
Figure 4-10 Stub Admittances

4-10
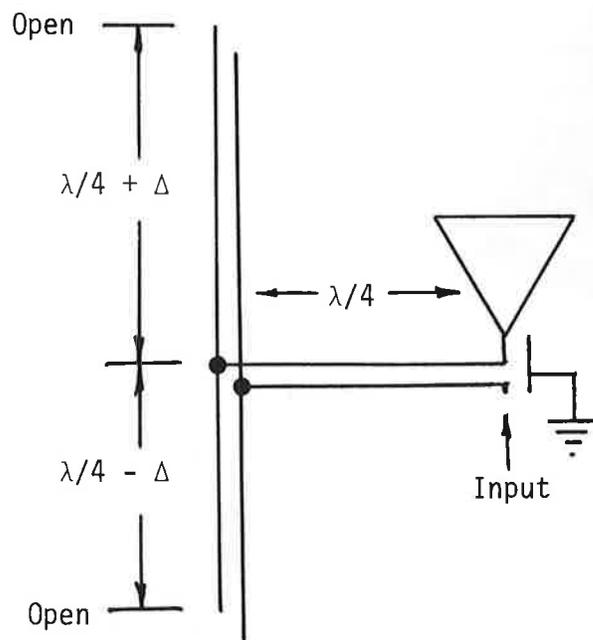
(a) Series Resonance Using Stubs in Parallel
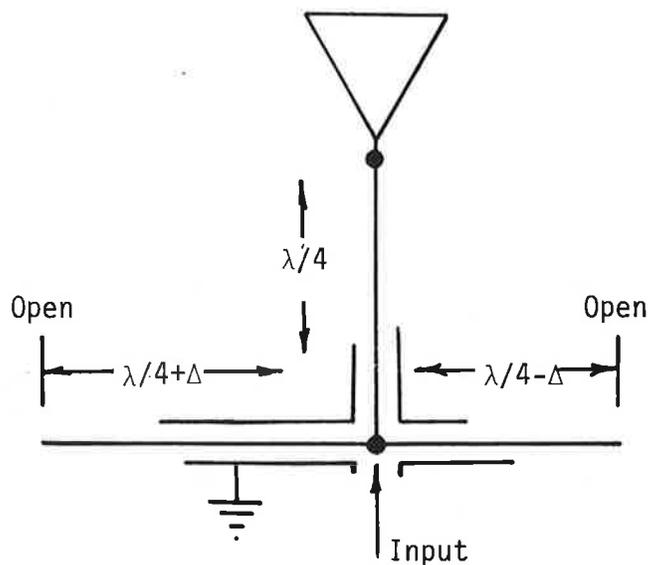
(b) Parallel Resonance

Figure 4-11 Circuits for Achieving Dual-Band Operation with Resonant Stubs
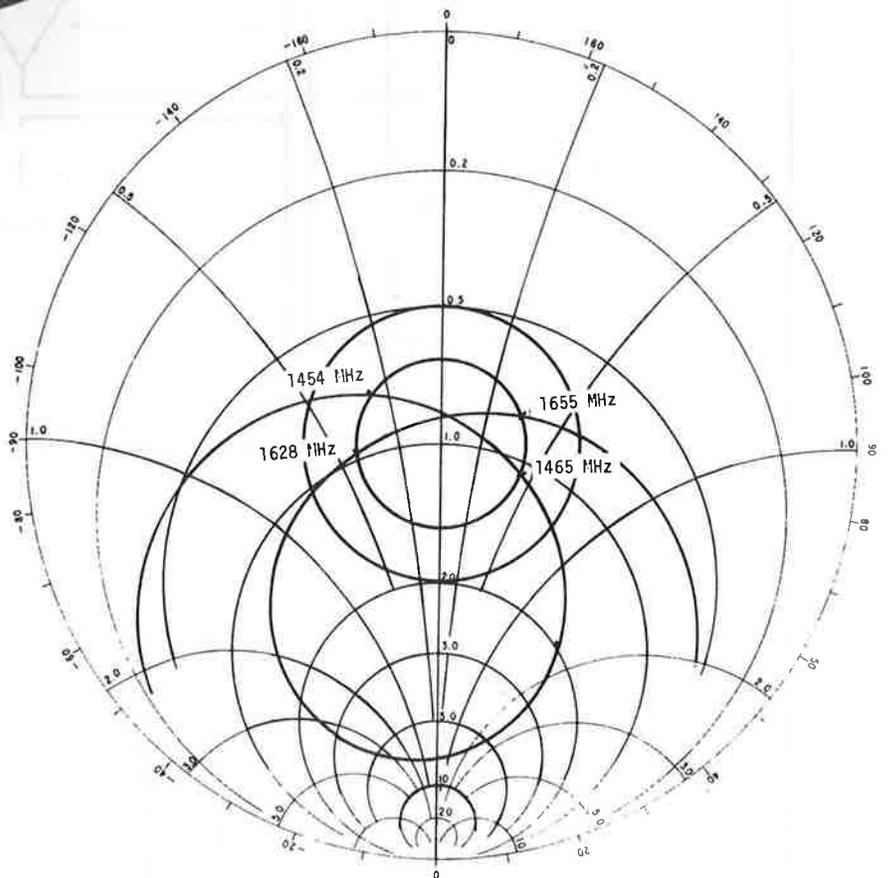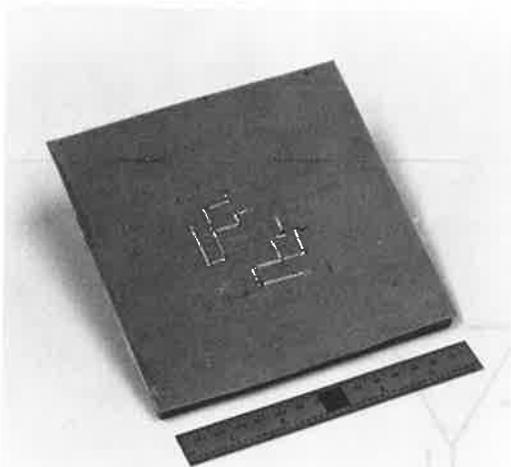
Figure 4-12   Stub Tuned, Dual-Frequency Single-Element Crossed Slot (Photograph
and Impedance Plot)

Resonant matching circuits for providing dual-frequency response are located
on a second substrate immediately above a 1/4-inch thick standard half-wave
microstrip radiating element. The photograph shows two resonant circuits
because the element is circularly polarized, and a separate circuit is required
for each linearly polarized component. The two resonant circuits were hand-
trimmed to obtain the match shown in the Smith plot. The two parts were then
connected to an external quadrature hybrid for pattern and gain measurements.
Measured gains in excess of 6 dB indicate that the added circuitry loss is
negligible.

The resonant circuit was found to be an effective way to achieve a dual frequency response on both the standard microstrip element and the crossed slot. It has the advantage of requiring only two substrate layers, a thick layer for the element and a thin layer for the feed. The primary disadvantage is the circuit's sensitivity to small changes in line length. Normal production tolerances would not be sufficient for reproducing the resonant circuits for 1/8" thick antennas. The circuit is less critical for thicker antennas and might be practical at 1/4". Increased thickness also improves the efficiency of the radiating elements.

4.4 BROAD BANDWIDTH ELEMENT

The third approach to making the antenna element operate in both the receive and transmit bands is simply to extend the basic bandwidth of the element. The percent bandwidth required is less than 7.5%, which can be achieved with a microstrip radiator. The basic approach investigated was to make the element volume larger, either by physically increasing the thickness or by dielectric loading. This approach is very simple to implement and was considered worth pursuing for this reason. Antennas based on this approach are shown in Figures 4-13 to 4-19: in some of these the use of dielectric loading is combined with integration of a broad-band microstrip quadrature hybrid. Some improvement in radiation efficiency at the receive and transmit bands was noted for these elements but performance was marginal compared with that of stacked elements.

All the working models exhibited significant gain roll-off at the ends of the extended bandwidth. However, the operating frequencies are located at the edges of the element bandwidth. For a standard microstrip element, the problem of gain roll-off can be alleviated by increasing the thickness of the element. But, as the element becomes more like the usual cavity-backed crossed slot, the bandwidth appears to depend less on thickness and more on slot dimensions. Slot dimensions, and particularly slot length, are limited by the space available in the array matrix.
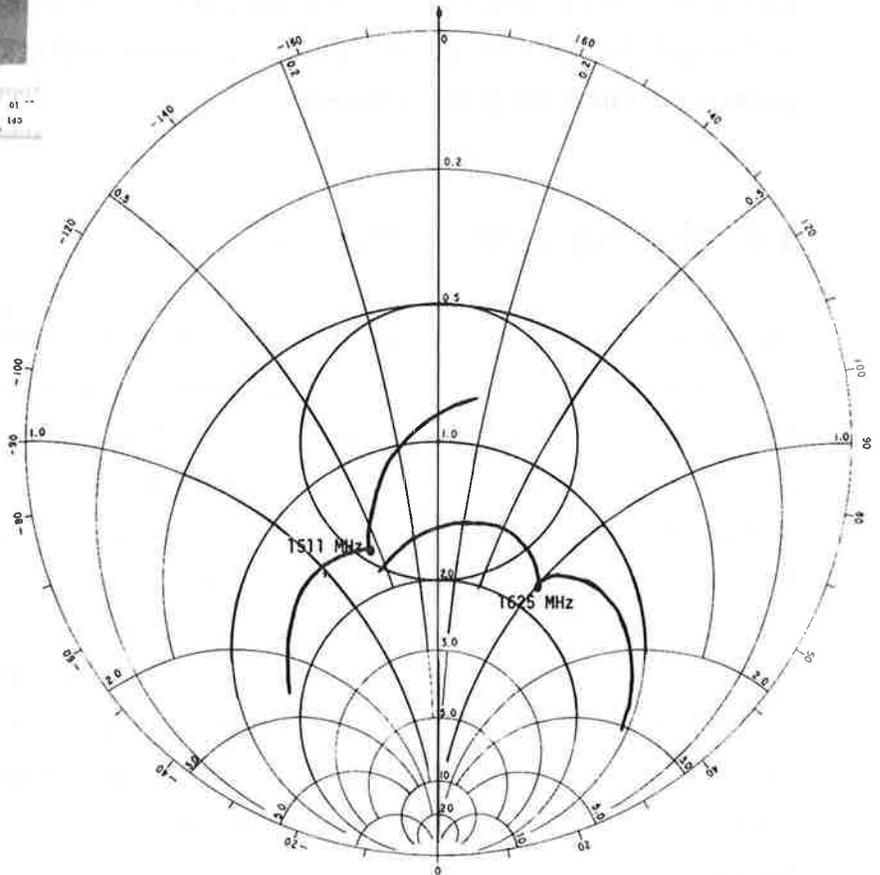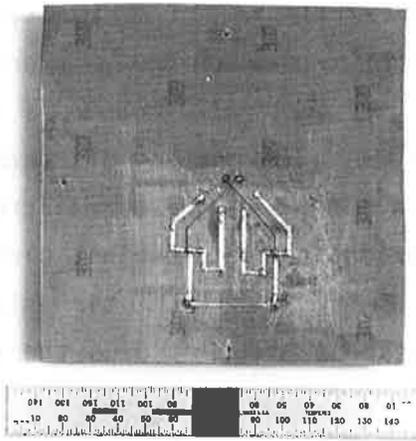
Figure 4-13 Second Version of the Stub-Tuned, Dual-Frequency Single-Element
Crossed-Slot Antenna (Photograph and Impedance Plot)

Resonant matching circuits are located on a substrate laminated to the top of a
1/8-inch thick crossed slot. Again two circuits are required, one for each
linearly polarized component. The two circuits are fed from a common feed point
with a 90^0 phase differential; no external hybrid is required. The impedance
plot shows the dual frequency response, though this has not been optimized. The
gain for this element was about 1 dB lower than other microstrip elements,
partly because of the non-optimized impedance and also because the 1/8-inch
thick cavity should have been a little thicker to maintain efficiency across
the band.
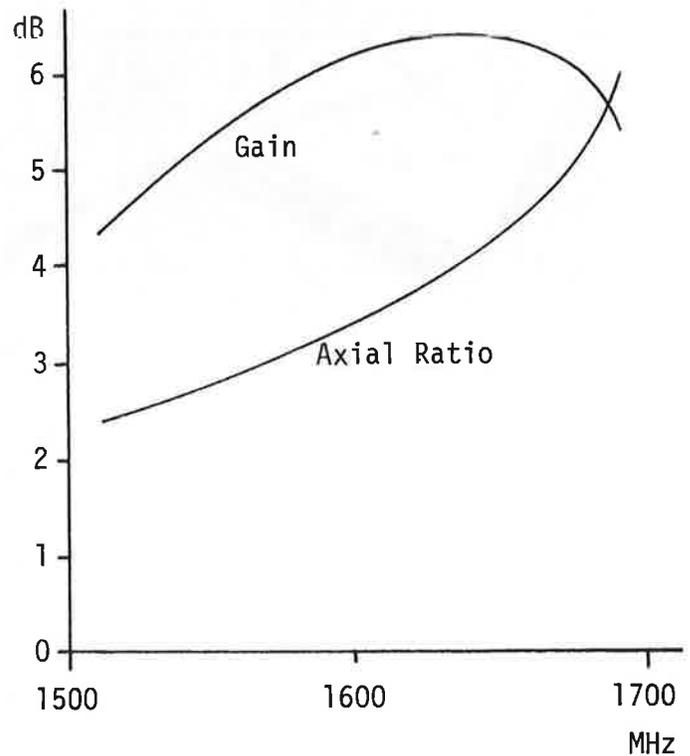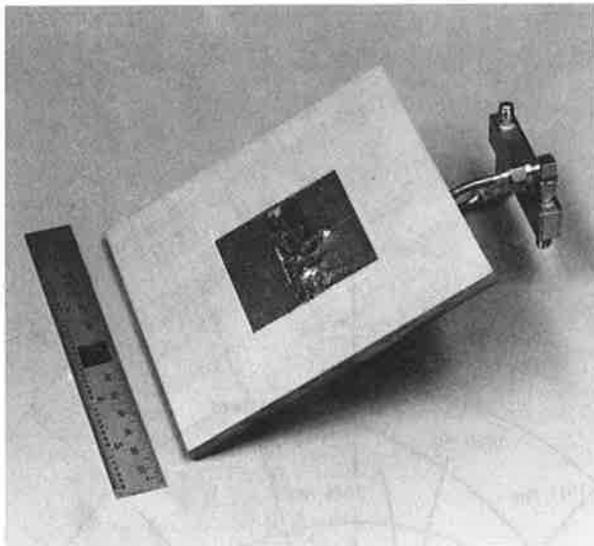
Figure 4-14 Broadband Single Microstrip Element (Photograph and Characteristics)

The broadband capabilities of a single standard microstrip element etched on 1/4-inch Teflon-Fiberglass board material were investigated first. The element was sized to resonate at 1,601 MHz which represents a center frequency between the allocated aeronautical satellite transmit and receive bands (1,543.5 - 1,558.5 MHz and 1,645 - 1,660 MHz). The VSWR at the center frequency was about 1.3:1. The element was fed with a commercially-available 3 dB directional coupler (90º hybrid). This technique provided a broadband 0 and 90º feed applied directly to the element through coaxial cables and connectors rather than by a microstrip feed network. With the directional coupler attached, the VSWR looking into the coupler varied from 1.1:1 at 1,543 MHz to 1.4:1 at 1,660 MHz.

Gain and axial ratio were measured over a range of frequencies from 1,525 MHz to 1,675 MHz as shown on the graph. The mediocre axial ratio is a result of the poor isolation between the linearly polarized components of the element. This can be corrected with a modified feed circuit. More significant, however, is the loss of gain at the edges of the extended band.

The power fed to the antenna at the band edges is being dissipated in the resistive port of the hybrid. For this design approach, some improvement in band-edge gain can be achieved by increasing the element thickness.

4-15
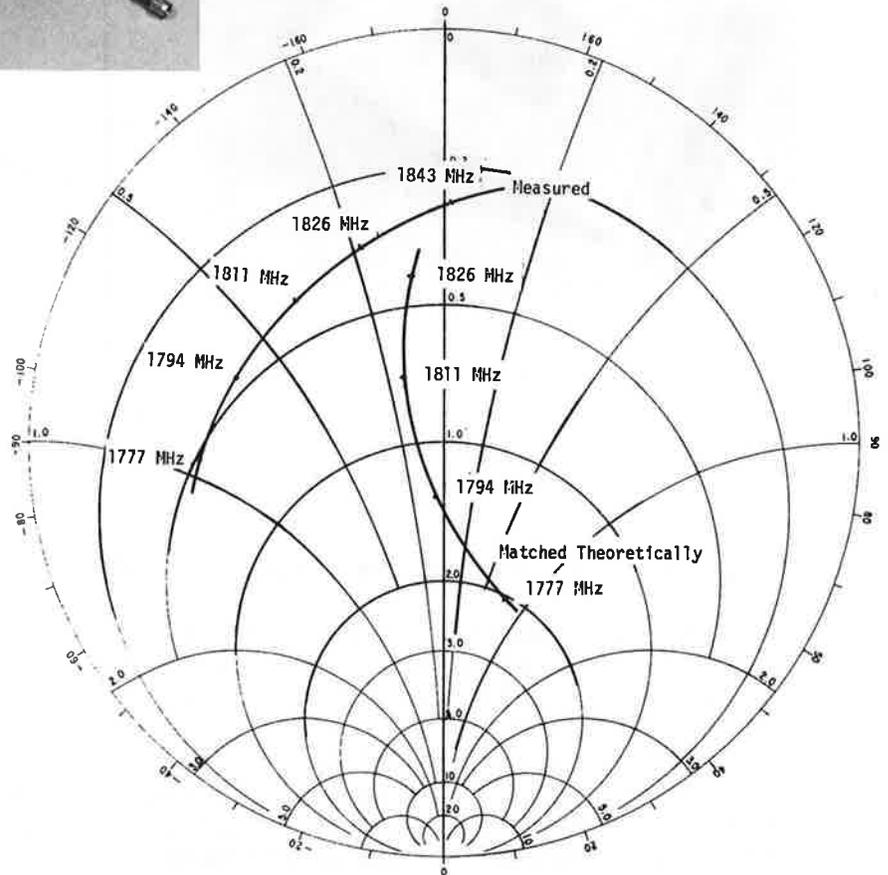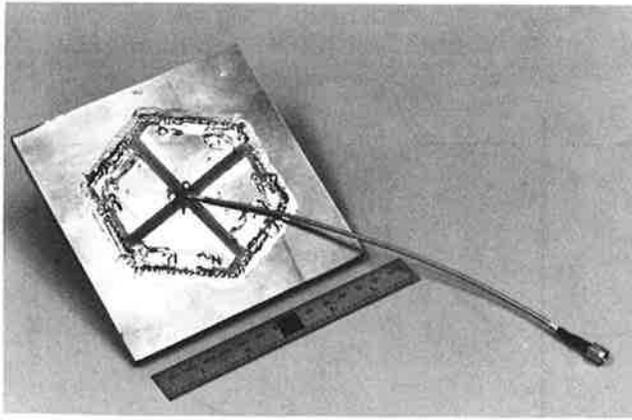
Figure 4-15   One Version of a Broad-Band Crossed-Slot Element (Photograph and
Impedance Plot)

Results similar to those for the microstrip element were obtained with various
crossed-slot configurations. This cavity-backed crossed-slot was fabricated on
1/4-inch Teflon-fiberglass. It was designed with a hexagonal cavity to maximize
the cavity volume in a triangular array matrix. Within the restricted space
available the slots were found to be too short to operate at the desired fre-
quencies. Therefore, it was necessary to load the ends of the slots by cutting
slot extensions as shown on the photograph. Although the correct resonant fre-
quency was obtained, the bandwidth does not appear to be capable of covering
both receive and transmit frequencies any better than the standard microstrip
element described in Figure 4-13. This is indicated by the impedance plot. The
entire 7-1/2% bandwidth would have to fall within a VSWR of 2:1 in order to
limit the gain roll-off to 0.5 dB.
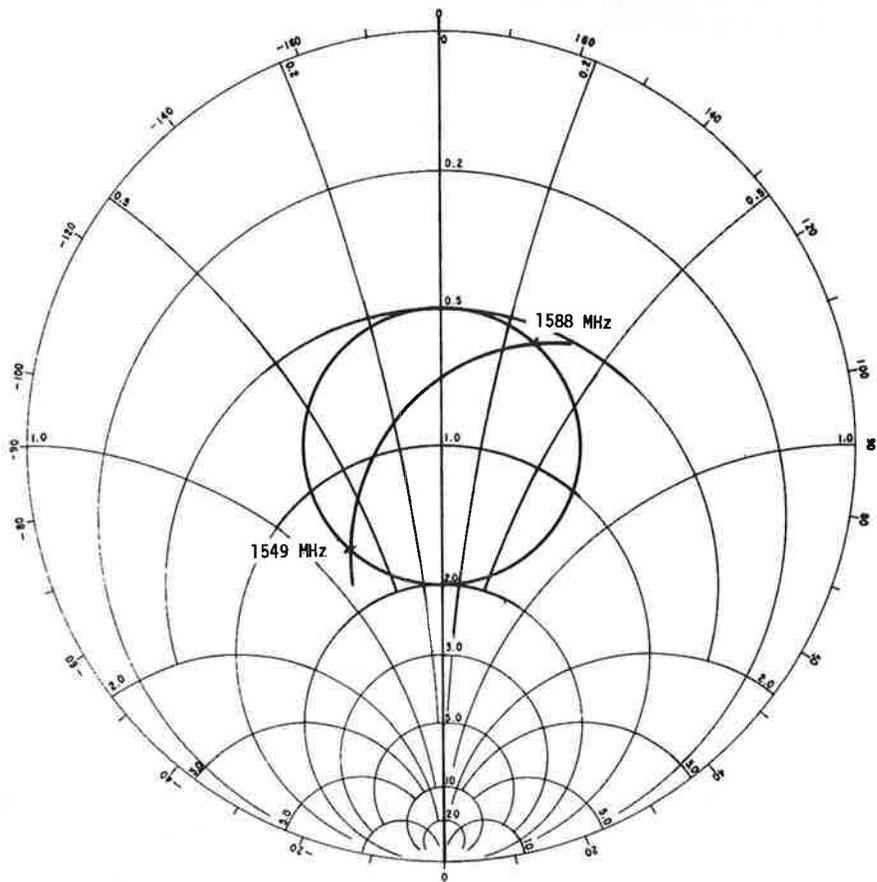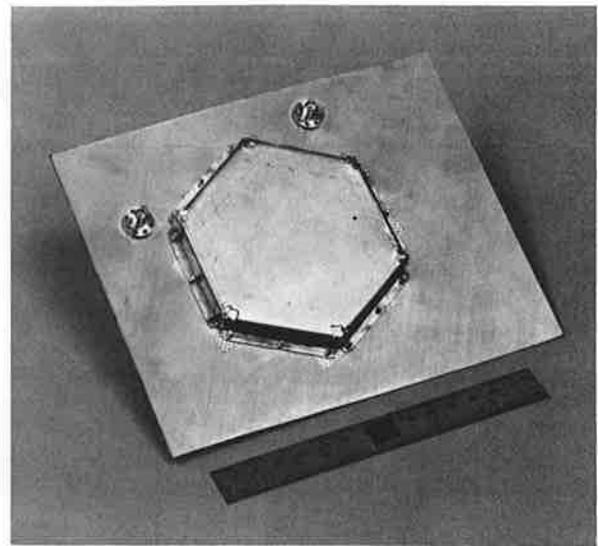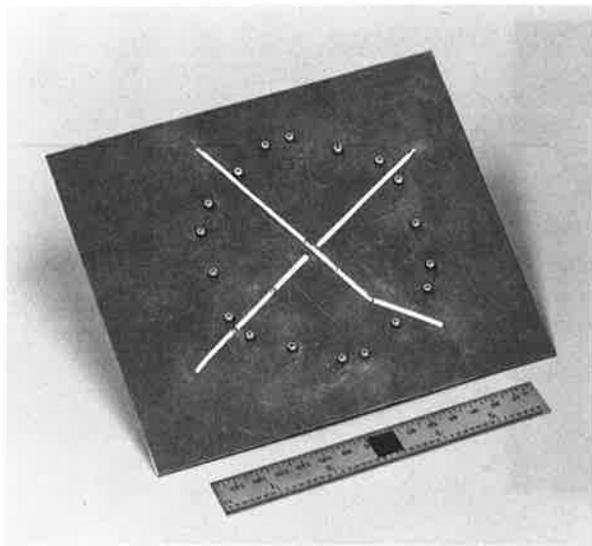
Figure 4-16   Broad-Band, Air-Filled, Crossed-Slot Element (Photographs and Impedance Plot)

This crossed-slot with air-filled cavity has microstrip matching stubs on the outer surface of the antenna. The impedance bandwidth is again too narrow to restrict the gain roll-off to less than 1 dB.
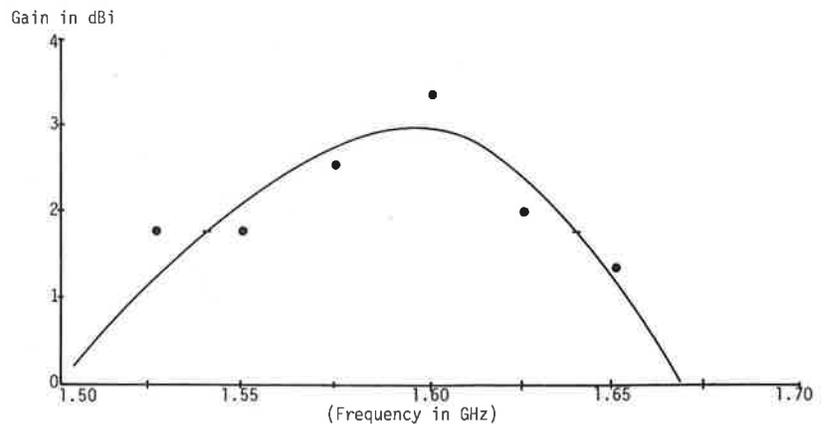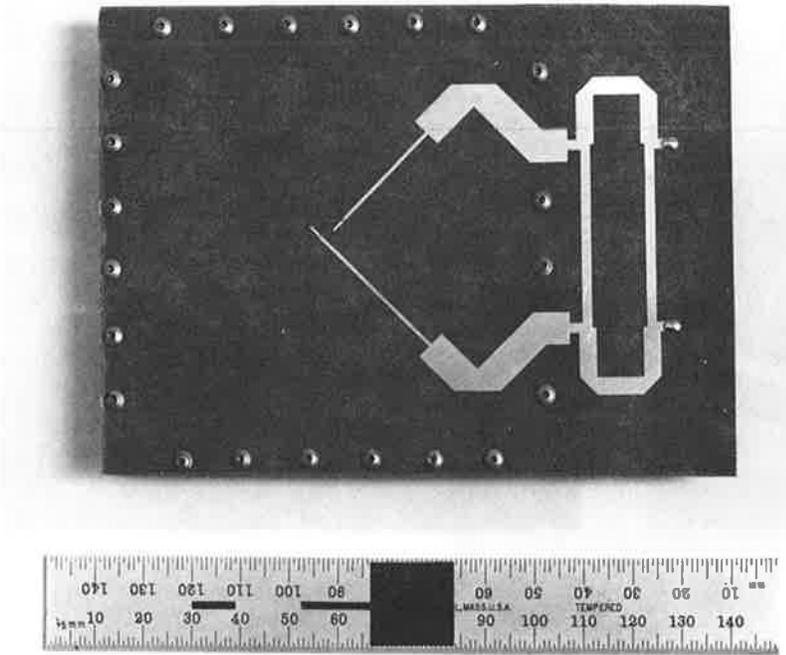
Figure 4-17 First Version of the Microstrip-Fed Broad-Band Crossed-Slot
Element(Photograph and Gain Plot)

All of the previous broadband designs used external quadrature-hybrids. To
demonstrate how the hybrid might be incorporated into a practical crossed-slot
design, this and several other elements using microstrip quadrature-hybrids
were developed. The 3/8-inch thick cavity was filled with paraffin because of
its desirable electrical properties (dielectric constant and loss tangent) and
easy workability. Radiation patterns are symmetrical and very much like the
patterns of all the other crossed-slot elements. The element is efficient, as
indicated by the center frequency gain of just over 3 dB. The plot of gain as
a function of frequency, shows that gain drops just over 1 dB at the limits of
a ±58 MHz bandwidth. This performance is in accordance with the earlier
results.

Gain in dBi
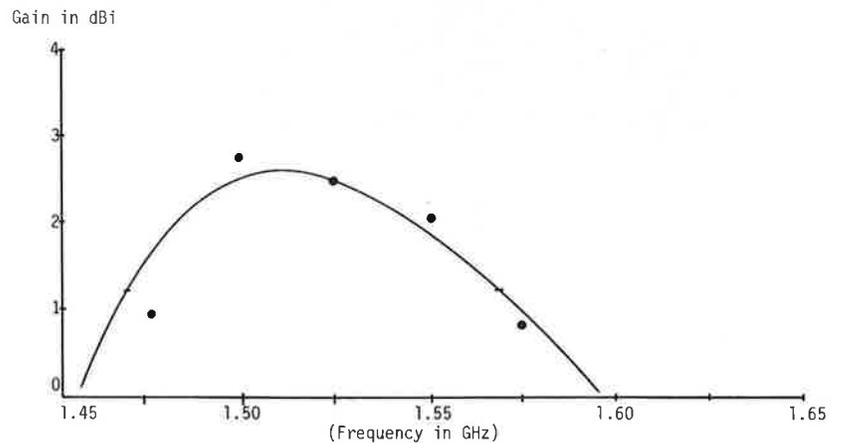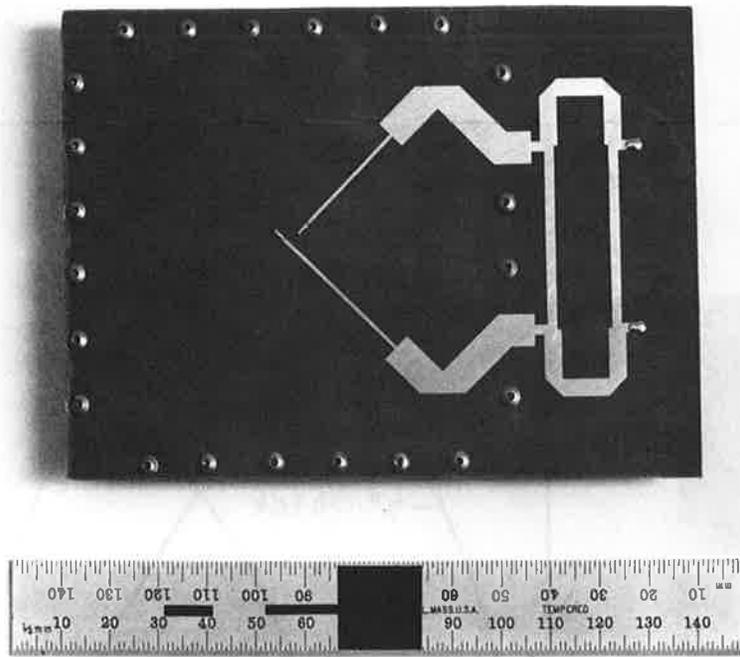
Figure 4-18 Microstrip-Fed, Dielectrically Loaded Crossed-Slot Element
(Photograph and Gain Plot)

To make the paraffin-loaded element a more practical device, the paraffin was
replaced with Emerson & Cuming TPM-4 casting resin. The metal cavity was over-
filled with resin which was machined flush with the cavity top after curing.
The interface between the TPM-4 and the crossed-slot circuit board was sealed
with Epon 828 resin and Versamid 140 hardener. The TPM-4 is a very low loss
material but the Epon 828 with Versamid 140 is not. Even with a small quantity
of the latter material, the gain of the element suffered. The plot shows the
gain of the element with frequency. The correction of the gain problem should
be possible with the exclusive use of TPM-4.
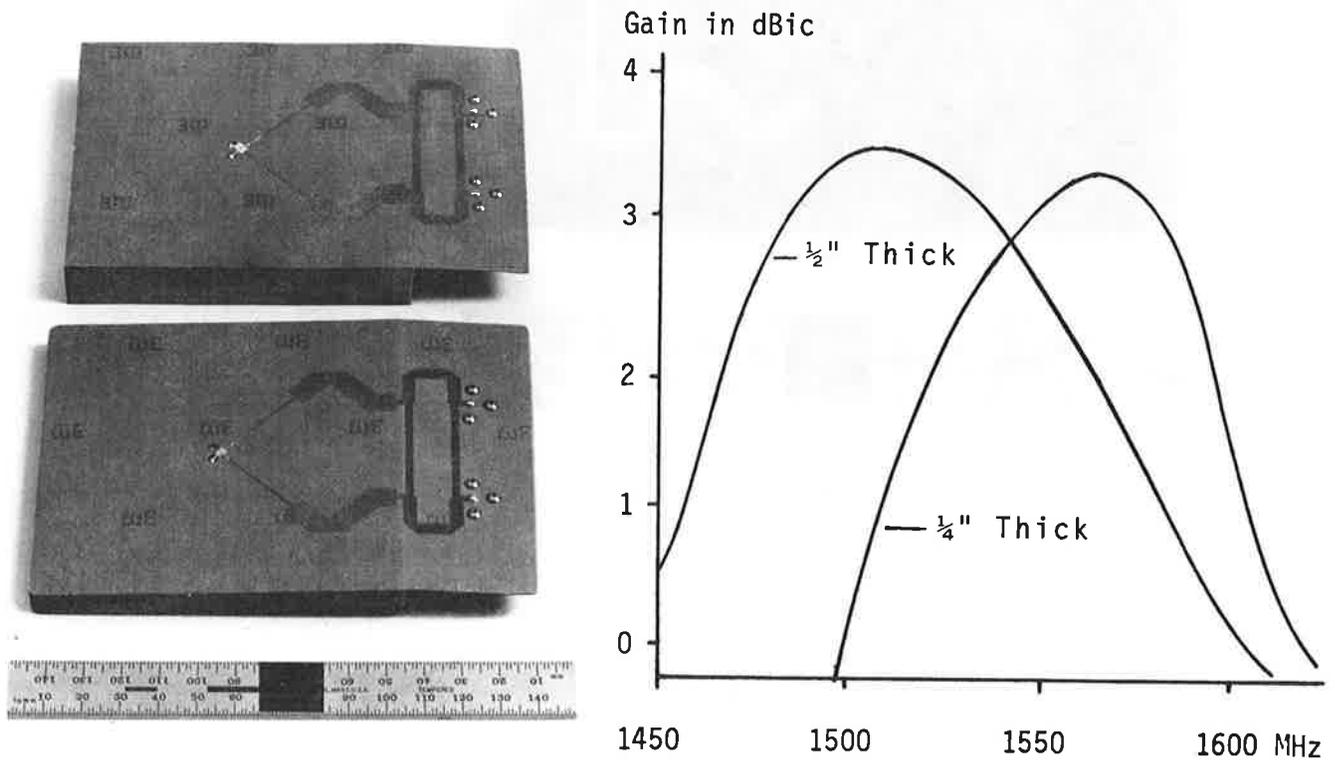
Figure 4-19 Microstrip Crossed-Slot Elements (Photographs and Gain Plots)

Microstrip crossed-slots were etched on 1/4-inch and 1/2-inch Teflon-fiberglass. Cavities were formed with plated-through holes as they would be in a production antenna of this kind. End loaded crossed-slots were etched in the top surface and fed across the slot from a thin (1/32-inch) circuitboard laminated to the top. A quadrature hybrid was incorporated into the design as it was in the two previous antennas (Figures 4-17 and 4-18).

After assembly, the antennas were tested for pattern and gain. The similarity between the gain versus frequency plots of the two is remarkable and disappointing. Doubling the thickness should have significantly increased the gain bandwidth. Evidently the bandwidth depends more on the slot length than cavity thickness. The slot length is limited by the array matrix.

5 ARRAY DEVELOPMENT

5.1 PHASED-ARRAY ANALYSIS

Most of the array development in this program was accomplished by model-ing. Predicting the effects of array phase and amplitude errors, however, was more efficiently done by analysis. Switched-line phase-shifters as described later are limited in broadband phased-array applications by step phase errors incurred in the zero phase state. To illustrate this situation consider the eight element array shown in Figure 5-1. The three-bit phase-shifters on each element are set for a progressive 90° phase variation across the array at f_0. Since the electrical length of the diode-switched delay lines varies directly with frequency, increasing the frequency to 1.1 f_0 will yield a new phase distribution as listed. The progressive interelement phase variation is now 99° with the notable exception that elements four and five differ by only 63°, a 36° phase error when compared to a 99° phase progression. The zero bit, or reference phase, remains zero degrees since it is independent of the differential increase in phase length of other lines.

The effect of this step phase error over an eight percent bandwidth was investigated by computer simulation for eight and sixteen element linear arrays. Three-bit phase-shifters and 0.6 wavelength element spacing were assumed. Patterns were computed for the arrays at 0.96 f_0, f_0 and 1.04 f_0 and with the beam steered to four positions between 0° and 40°. The results are tabulated in Table 5-1. Generally only minor variations were noted in array performance over this bandwidth. First side-lobe levels varied approximately ±1.5 dB about the positions at f_0, and the beam position variation was about ±1°. Based on this data it appears switched-line phase-shifters can be used effectively over an eight-percent bandwidth.

Another consideration is differential insertion loss in the phase-shifter and its effects on the array performance. Typically, minimum insertion loss occurs in the zero state, while the 45°, 90° and 180° bits exhibit an in-creased loss of 0.25, 0.15 and 0.05 dB respectively, over the zero state.

THREE-BIT PHASE SHIFTER

ELEMENT	PHASE F_0 (Degrees)	PHASE 1.1 f_0 (Degrees)
1	0	0
2	90	99
3	180	198
4	270	297
5	0	0
6	90	99
7	180	198
8	270	297
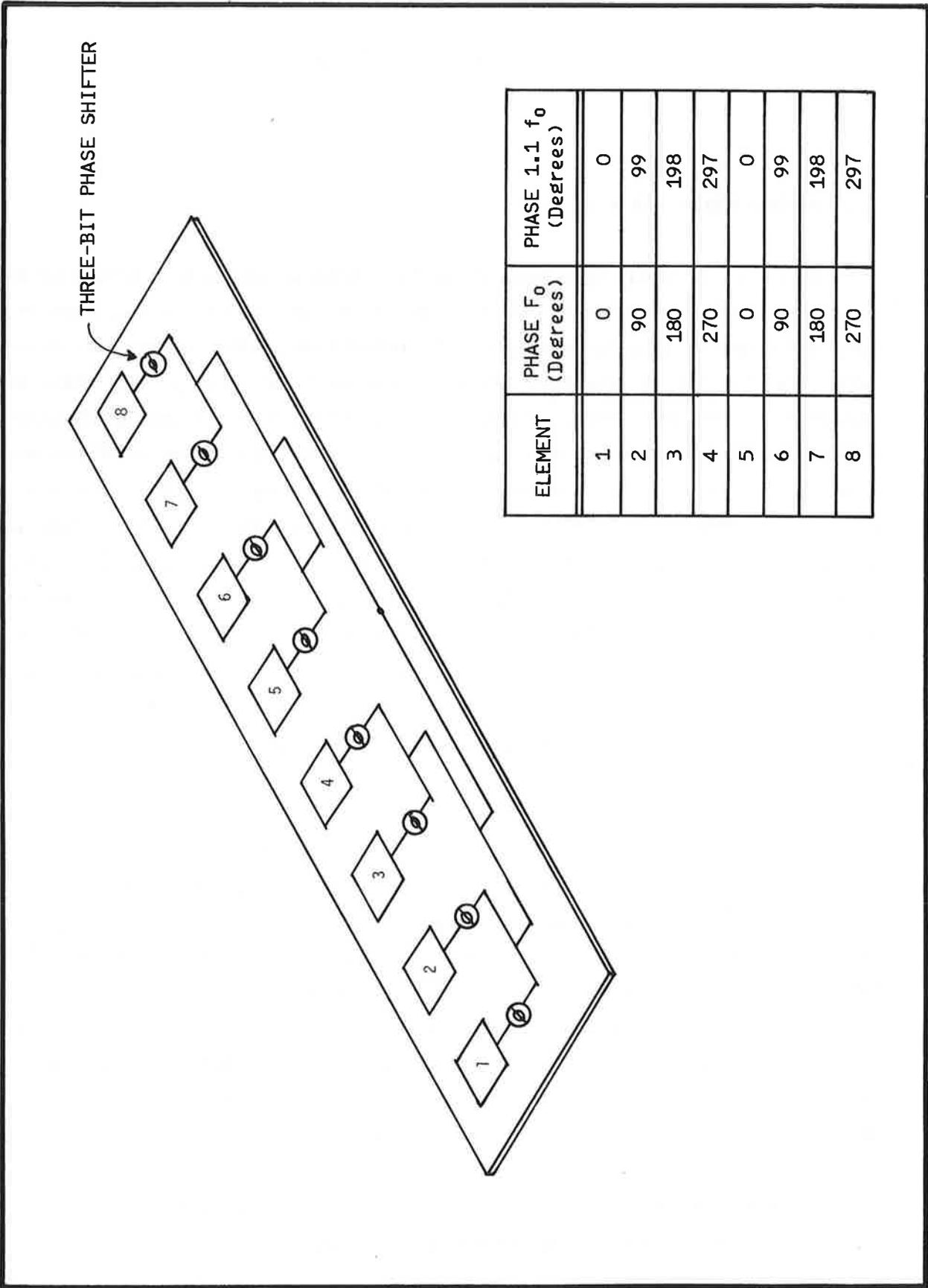
Figure 5-1 Array-Analysis Model

Table 5-1

SCANNED-ARRAY DATA SUMMARY

NUMBER OF ELEMENTS	ARRAY	FREQUENCY	PHASE PROGRESSION (Degrees)	BEAM POSITION (Degrees)	3 dB BEAMWIDTH (Degrees)	SIDELOBES Left Right		GRATING LOBE
Eight Elements	1	f_0	0	0	10.7	13.1	13.1	
		$0.96\ f_0$	0	0	11.0	13.1	13.1	
		$1.04\ f_0$	0	0	10.3	13.1	13.1	
	2	f_0	45.0	12.2	10.7	13.9	12.6	
		$1.04\ f_0$	46.8	12.2	10.2	13.8	12.7	
	3	f_0	90.0	24.5	11.5	15.4	12.2	
		$0.96\ f_0$	86.4	25.5	12.0	17.4	10.6	
		$1.04\ f_0$	93.6	23.7	11.4	13.8	13.5	
	4	f_0	135.0	37.7	13.0	18.4	11.0	-9.0
		$0.96\ f_0$	129.6	39.2	13.7	19.6	10.5	-8.0
		$1.04\ f_0$	140.4	36.5	12.5	17.5	11.5	-8.0
Sixteen Elements	5	f_0	45.0	12.5	5.5	13.5	13.0	
		$1.04\ f_0$	46.8	12.3	5.3	12.2	14.5	
	6	f_0	90.0	25.0	5.7	14.0	12.5	
		$1.04\ f_0$	93.6	24.0	5.5	13.5	13.0	
	7	f_0	135.0	38.7	6.7	15.5	12.0	-11.8
		$1.04\ f_0$	140.4	37.5	6.5	14.5	12.5	8.5
Sixteen Elements with Amplitude Variations	8	f_0	45.0	12.5	5.5	14.0	13.0	
	9	f_0	90.0	25.0	5.8	15.3	12.4	
	10	f_0	135.0	38.7	6.7	17.2	11.0	12.1

Simulating expected losses for the various phase distributions indicates negligible impact on pattern performance. The sixteen element case, the worst condition, is also included in the table.

Although no appreciable pattern degradation is encountered, gain will be approximately 1 dB lower than theoretical due to phase-shifter loss. This value can approach 1.5 dB for various phase shifter combinations. To compensate for directivity loss in maximally steered beams, it would be advantageous to introduce constant-phase delay lines in front of the phase-shifters such that all phase-shifters could be in the minimum insertion-loss state (zero state) for the beam steered closest to the horizon.

5.2 PHASED-ARRAY MODELING

One of the goals of the program was to develop the capability for nearly hemispherical scanning coverage of the medium-gain beam. This means that the array must go completely to an end-fire mode, since ground plane effects will always force the beam up 10° to 20°. The easiest way to avoid a bi-directional end-fire pattern is to space the elements a quarter wavelength apart, but this is not possible in a linear or rectangular array with elements that are a third to a half-wavelength square. In this case, it is necesary to locate the elements on a triangular grid, three examples of which are sketched in Figure 5-2. Figure 5-2 is an attractive approach because phase shifters can be located on either side of the array, and there is no congestion of elements and phase shifters even though the elements are very close together. A static model of this array with temporary coaxial feed is shown in Figure 5-3. The model is built so that elements may be rotated to change their relative phase. The elements are the standard microstrip elements rather than the broader-beamwidth microstrip crossed-slot element. Even so, the end-fire pattern comes quite close to the horizon. Using the crossed-slot in this array should permit somewhat higher gain levels near the horizon. Figures 5-4 and 5-5 show two radiation patterns recorded for this antenna. An array of this kind could be mounted on the top centerline of an aircraft and steered in the roll lane, as well as the pitch plane.
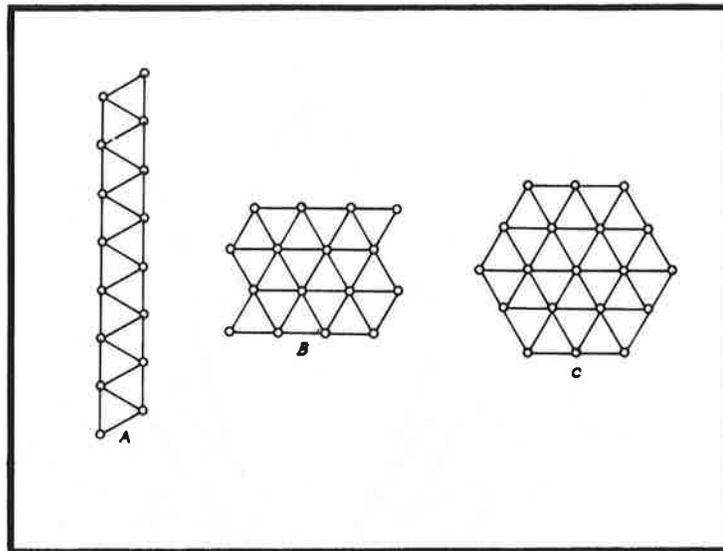
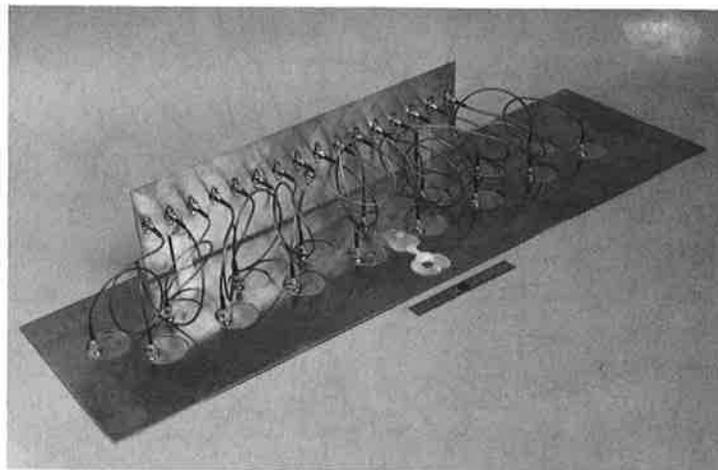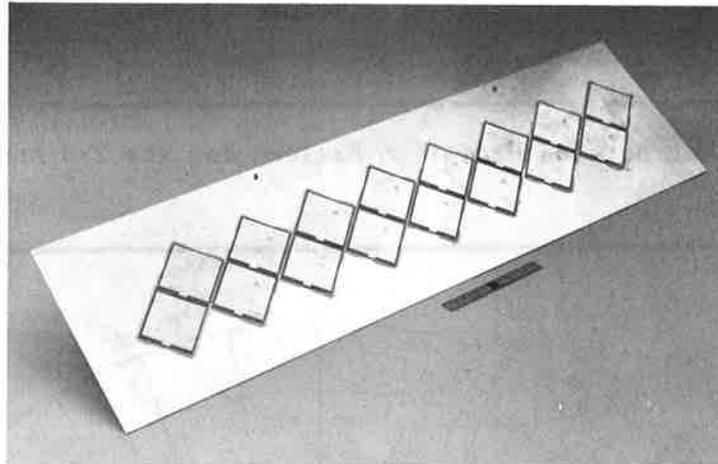Figure 5-2 Three Triangular-Array Matrices

Figure 5-3 Static 2x8 Array Model, Front and Back Views
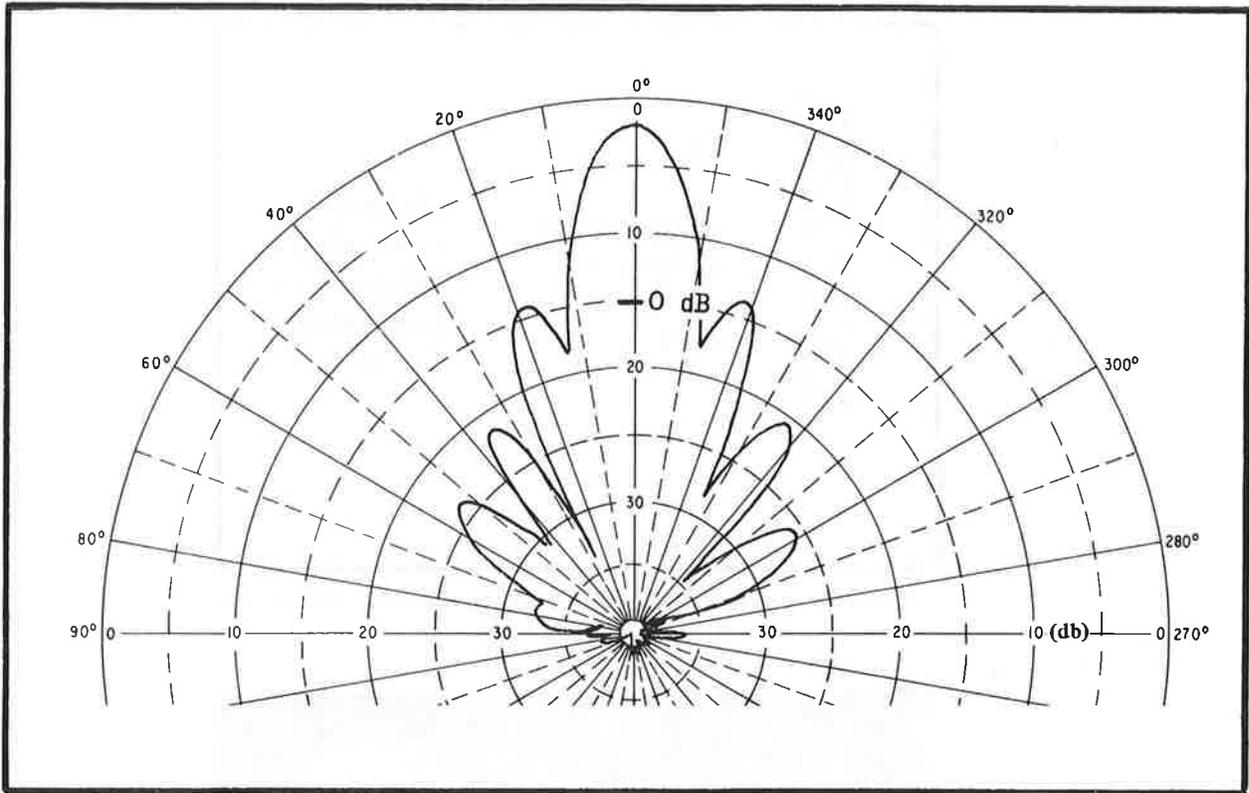
Figure 5-4 Broadside Radiation Pattern for the 2x8 Array Model
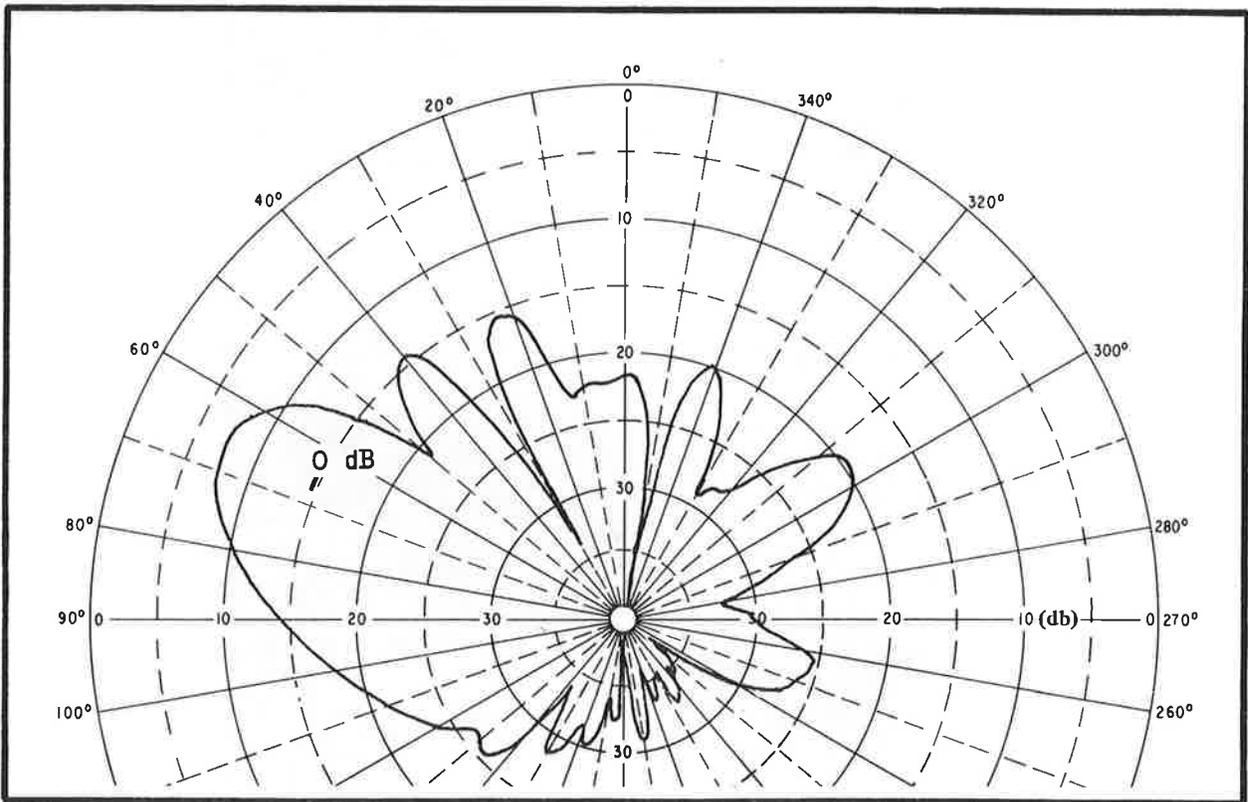

Figure 5-5 End-Fire Radiation Pattern for the 2x8 Array Model

The disadvantage of the 2x8 array is that the loss of gain at end-fire is greater than necessary. Mailloux (see bibliography) has shown that the ratio of gain at end-fire to gain at broadside (with a perfectly conducting ground) is given by:

$$\frac{D}{D_0} = \left(\frac{C\lambda}{\pi L_1}\right)^{1/2}$$

where L_1 is the array length in the end-fire direction and C is a constant which varies from 3.5 to 7 depending upon phase velocity and the array distribution. It can be seen that for a given broadside gain scan loss is minimized by decreasing L_1 as much as possible.

Mailloux's equation does not fully predict the 6 dB loss measured for the 2x8 array, but it does suggest a better array configuration. The aperture of an array that steers to end-fire in every azimuthal direction should be as small as possible in every direction. This means the aperture should preferably be a circle, and if not a circle, then a hexagon or square as in Figure 5-2c and 5-2b.

For these reasons a 4x4 array (Figures 5-6 and 5-7) was assembled and tested. It showed gains of 12 dBi at broadside and 9 dBi at end-fire. Patterns are shown in Figure 5-8 and 5-9 for the array on a flat ground plane. Figure 5-10 shows a pattern equivalent to that Figure 5-9 on a curved ground plane simulating the surface of a 747 aircraft. Notice that even though the broadside gain has been reduced slightly due to overlapping element apertures, the end-fire gain has increased significantly. The end-fire patterns do not show the large (cross-polarized) back lobe which, of course, detracts from the gain in the desired direction. Improved polarization purity does not seem to reduce this cross polarized lobe. In fact, polarization purity of the main lobe was actually quite good even at end-fire. Axial ratios on the order of 3 dB were measured as low as 10° from the horizon.

Previously described array modeling was done with standard microstrip elements rather than the newer microstrip crossed-slot. The main reason for developing the crossed-slot was to improve array performance at end-fire; it
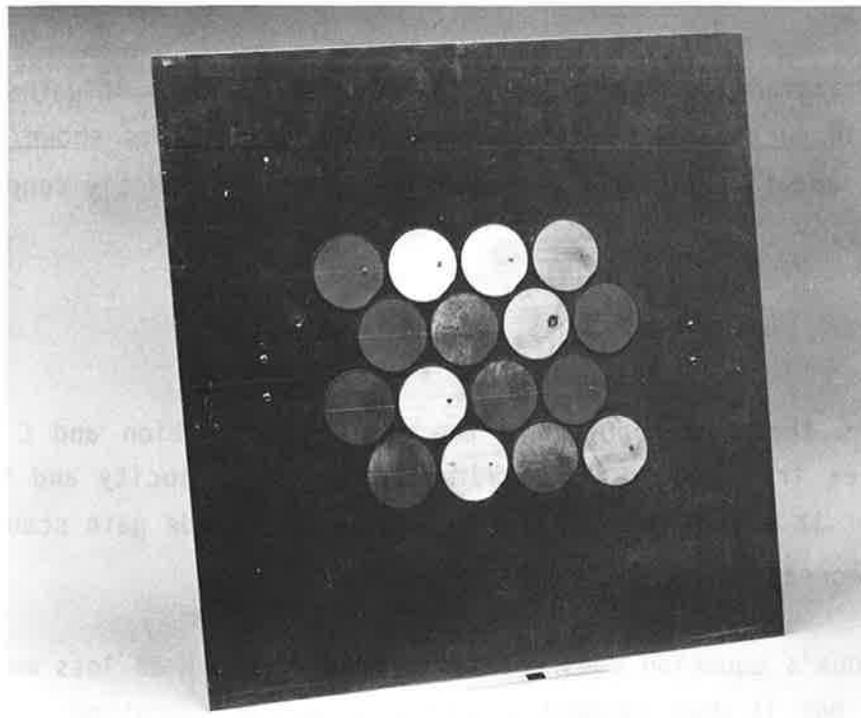
Figure 5-6 Static 4x4 Array Model Front View
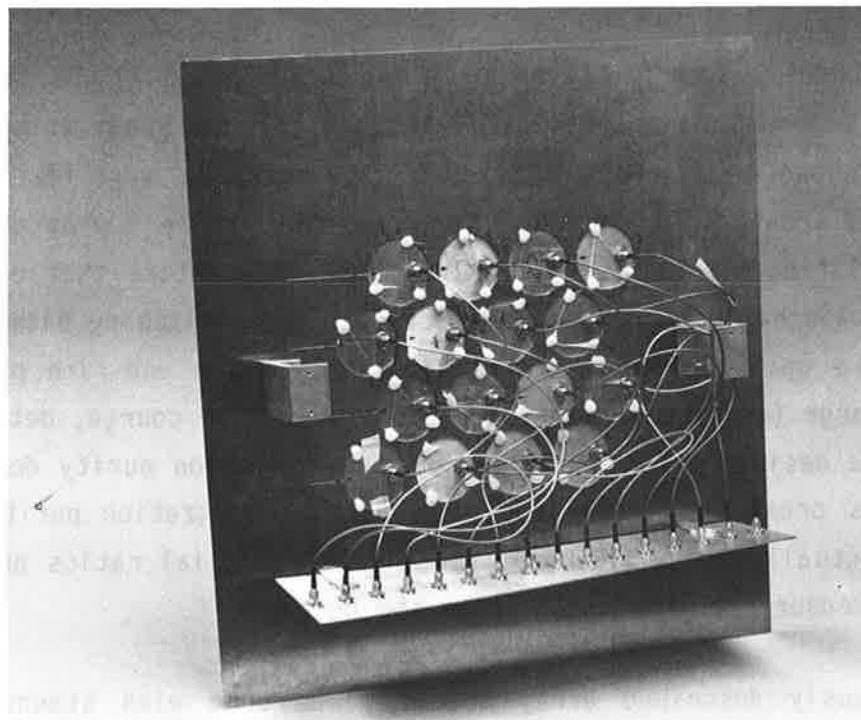

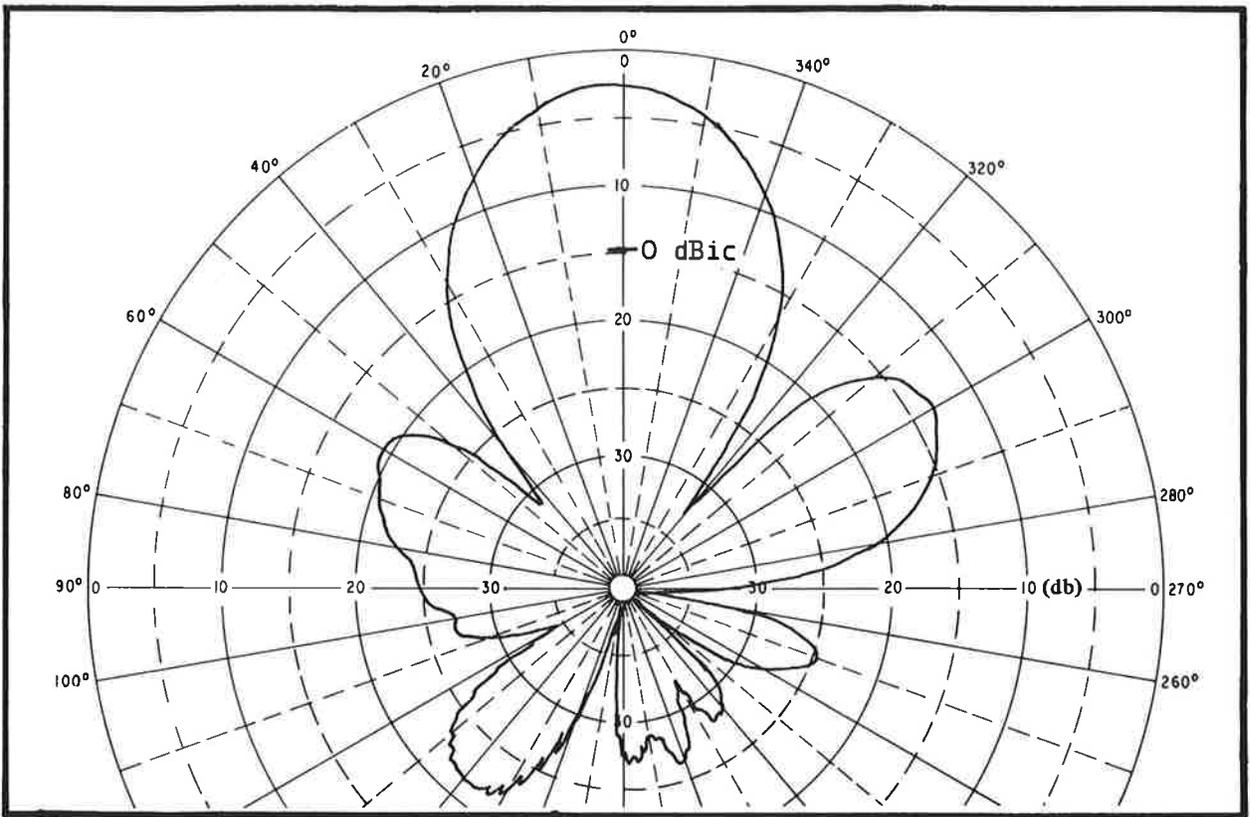Figure 5-7 Static 4x4 Array Model Back View, Showing the Coaxial-Feed Network

Figure 5-8   Broadside Radiation Pattern of 4x4 Array on 4-foot Square Ground
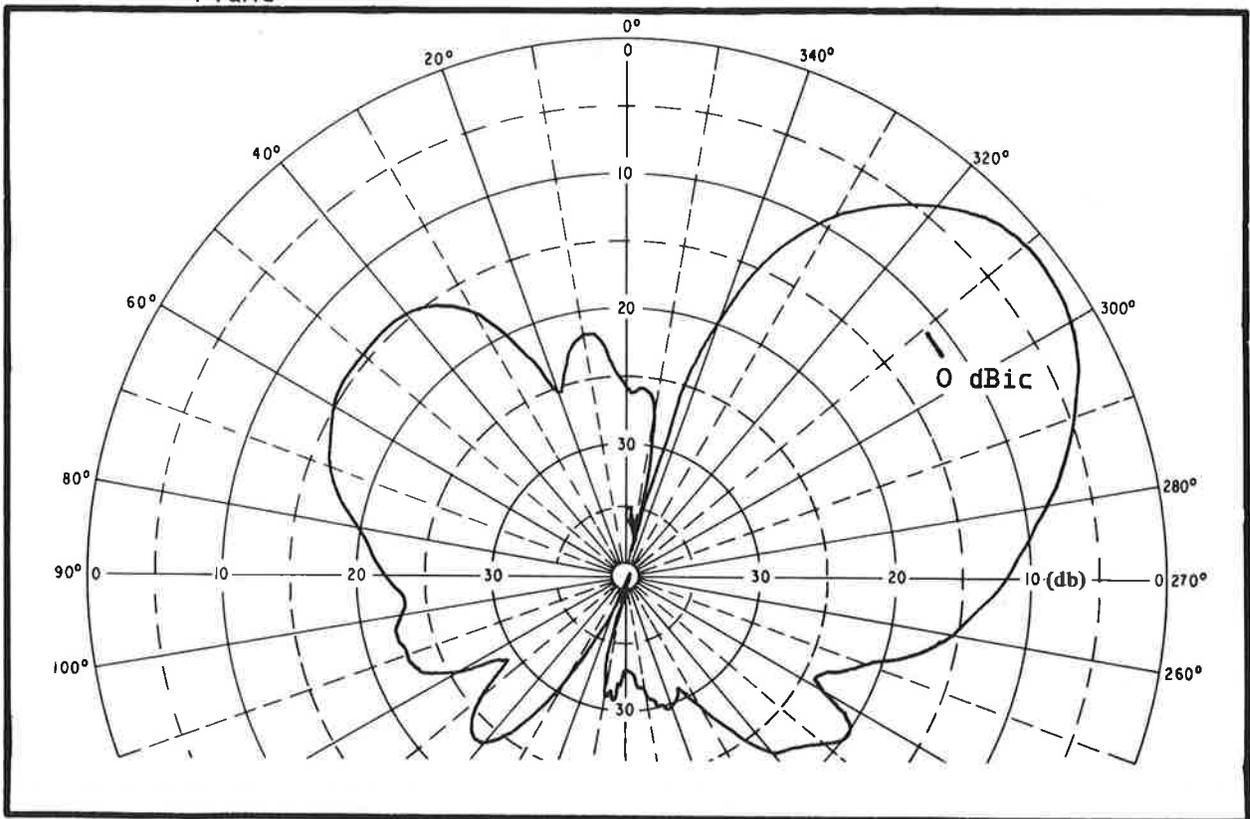Plane

Figure 5-9   End-Fire Radiation Pattern of 4x4 Array on 4-foot Square Ground
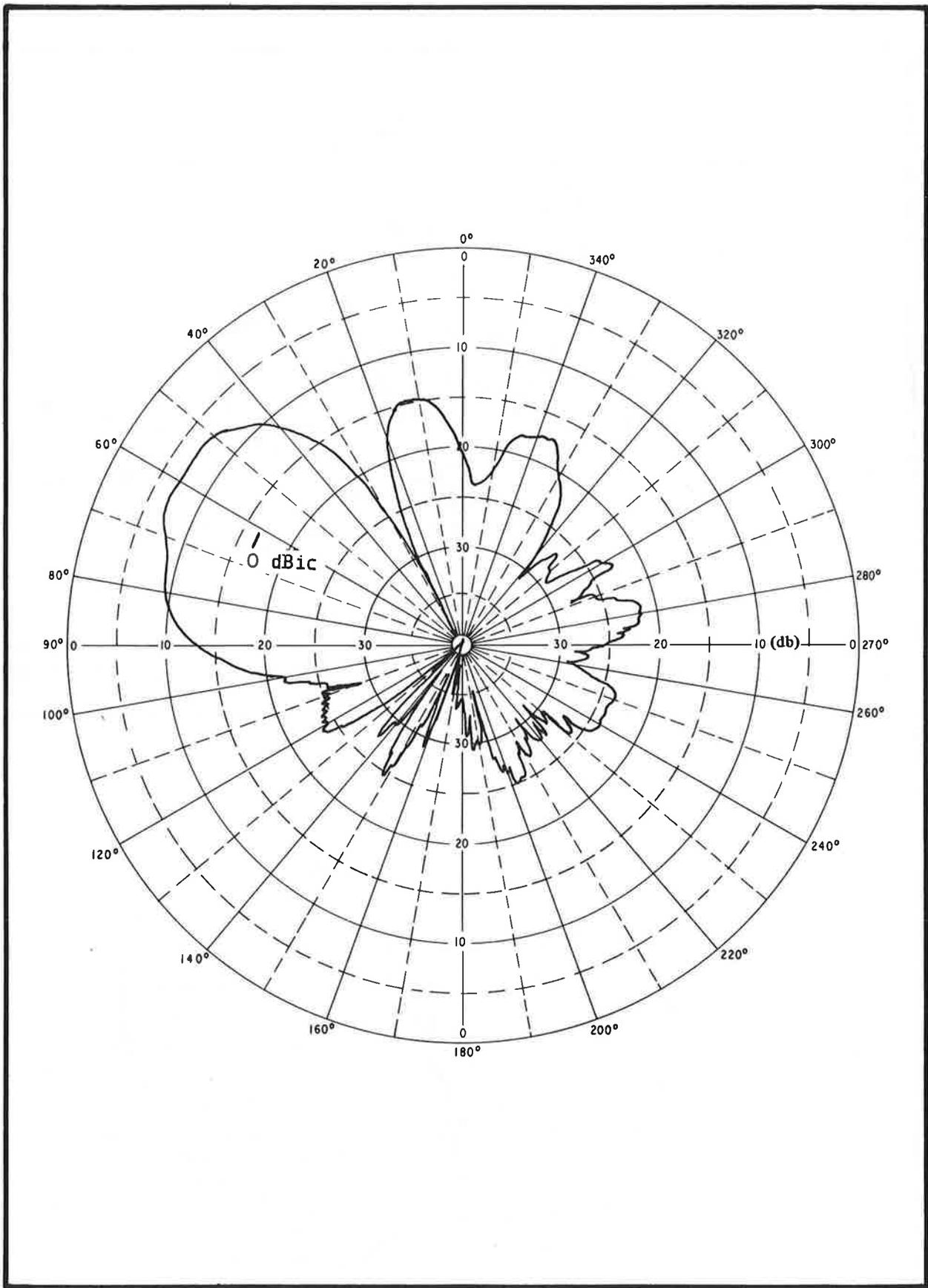Plane

Figure 5-10 End-Fire Radiation Pattern of 4x4 Array on Curved 4x8-foot Ground Plane

5-10

was necessary to model the array with crossed slots. A simplified single-frequency element was designed for this purpose. A typical pattern of this element is shown in Figure 5-11, and its impedance plot is shown in Figure 5-12. Unfortunately the feed for this element was lossy, and the resulting gain was about 2 dB less than that of the other microstrip crossed-slots. When the element was incorporated into the 4x4 array, the array gain was reduced by the same 2 dB. Radiation patterns and gain for the array, Figures 5-13 and 5-14, show an improvement only if 2 dB of additional gain is included. It is noteworthy that the ratio of broadside gain to end-fire gain was reduced to 2 dB. In addition, the cross-polarized back lobe was reduced. It can be concluded that an efficient crossed-slot element would indeed improve the performance of the array.

5.3 SWITCHED-ARRAY MODELING

Early in the program, consideration was given to switched arrays as an alternative to phased arrays. One switched-array concept included a cluster of end-fire arrays pointed in different azimuthal directions. The appropriate array would be switched on while the others were turned off. An end-fire array that could be used in this way was fabricated and tested. The model is shown in Figure 5-15, and the radiation pattern is shown in Figure 5-16. The array uses full-wavelength resonant elements for this experimental work to avoid the model fabrication problems associated with plated-through holes in quarter-wavelength elements. Although the array performed well, as Figure 5-16 shows, the basic concept seemed to offer no advantage over the phased array except a reduction in phase-shifter complexity and had the disadvantage of requiring a much larger surface area.

More recently the switched array has received some additional thought. There may be some simplification and cost reduction to be gained. The possibility of switching elements rather than complete arrays might permit coverage of the entire hemisphere in a reasonable amount of surface area. The switch for the antenna could conceivably have significantly fewer diodes than required for a phased array. The concept has already been successful in a
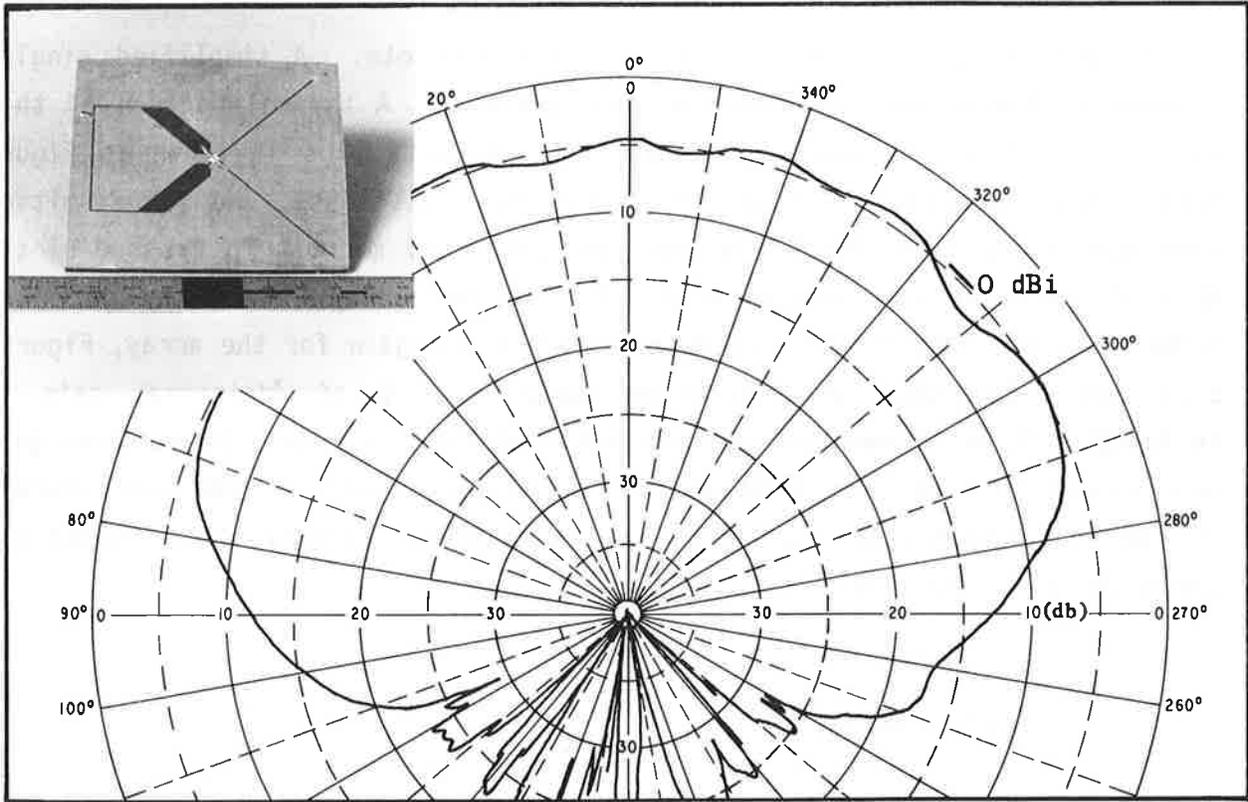
Figure 5-11 Single-Frequency Crossed-Slot Photograph with Radiation Pattern
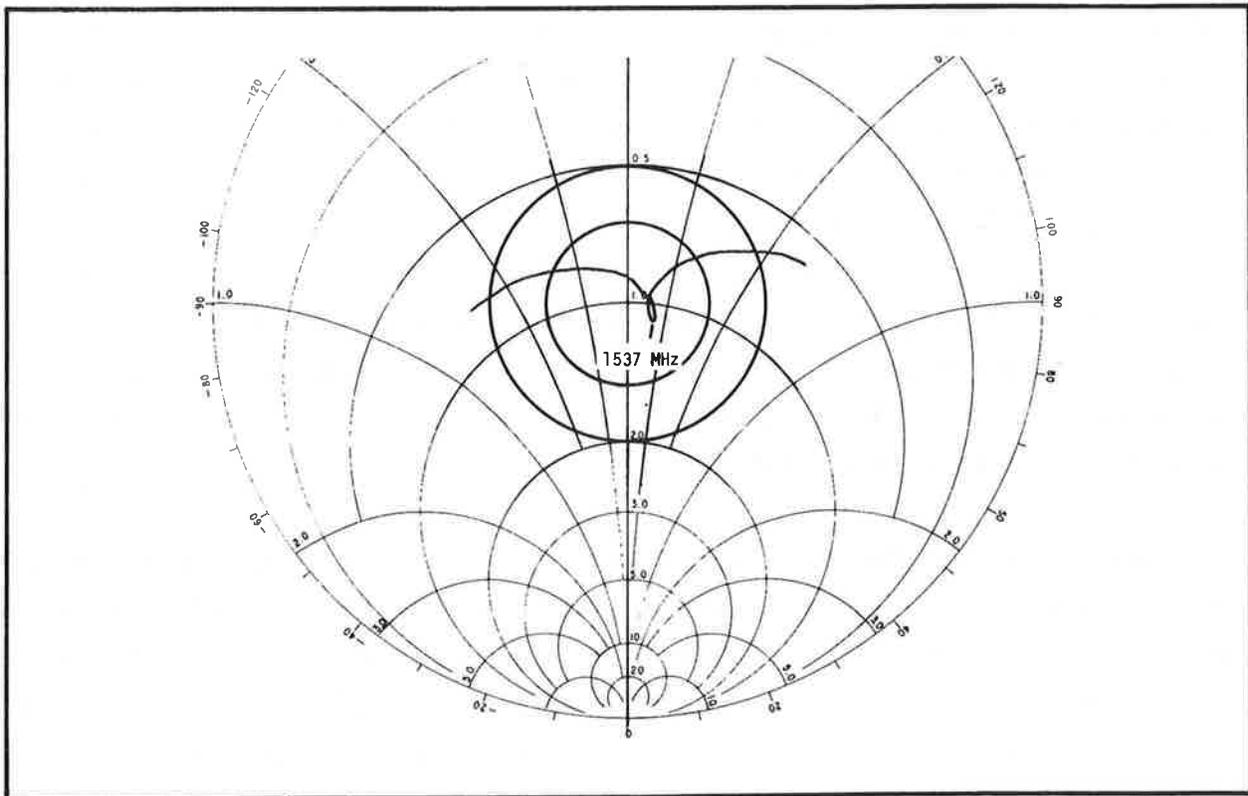
Figure 5-12 Impedance Plot of Single-Frequency Crossed Slot
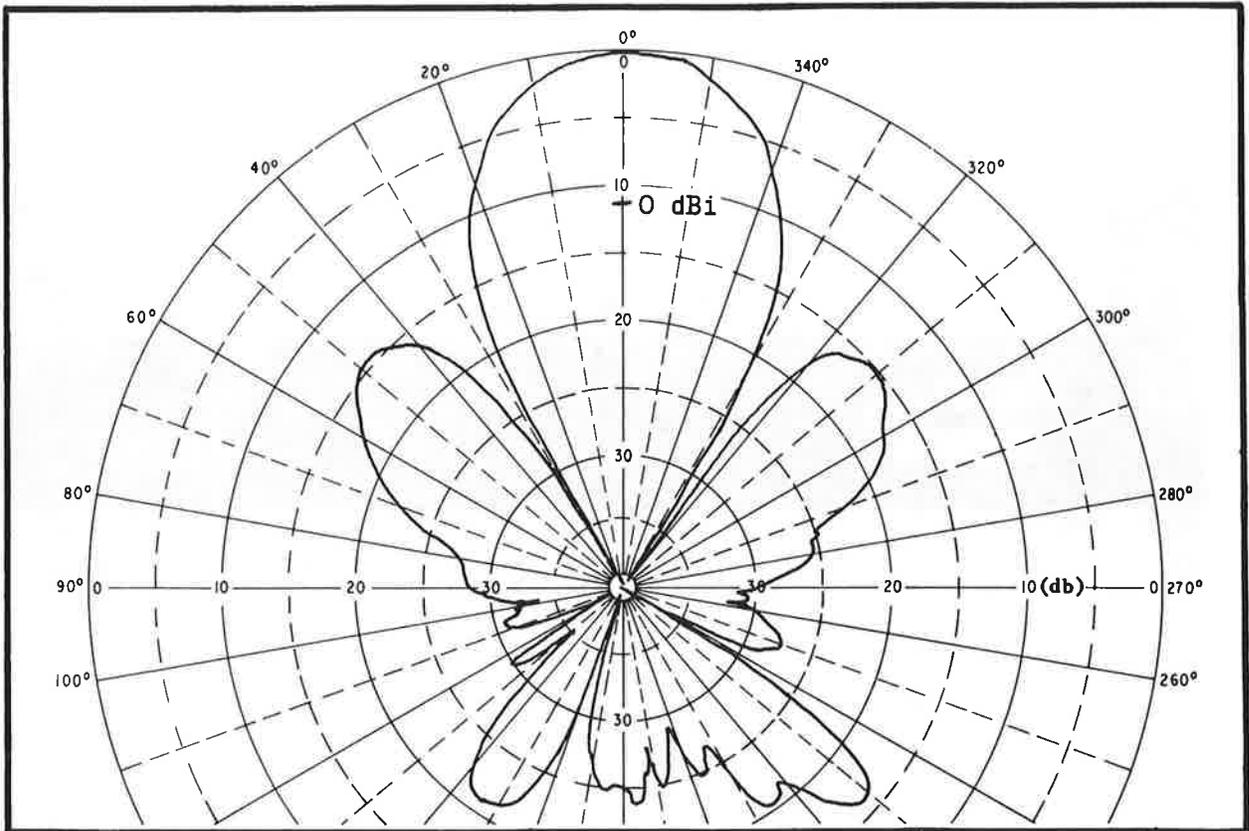
Figure 5-13   Broadside Radiation Pattern of 4x4 Array of Crossed Slots,
4x8-foot Ground Plane
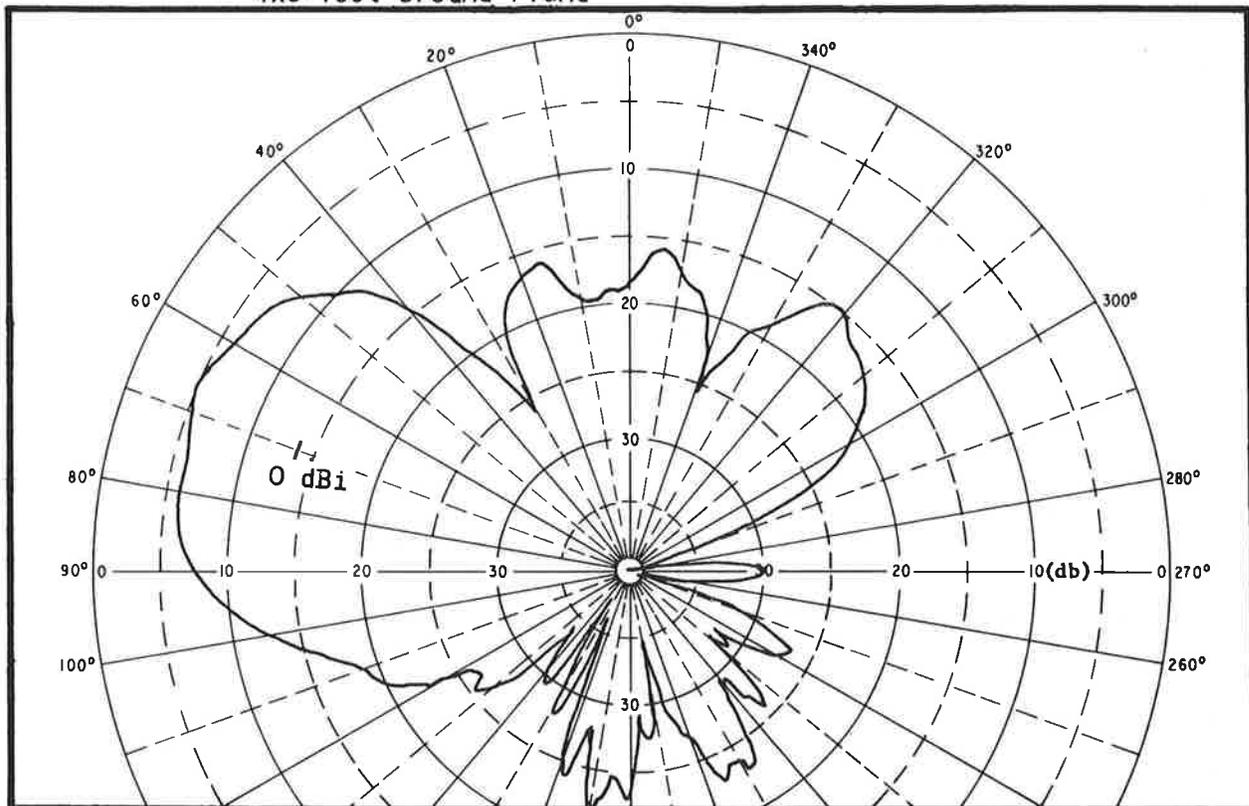
Figure 5-14   End-Fire Radiation Pattern of 4x4 Array of Crossed Slots,
4x8-foot Ground Plane
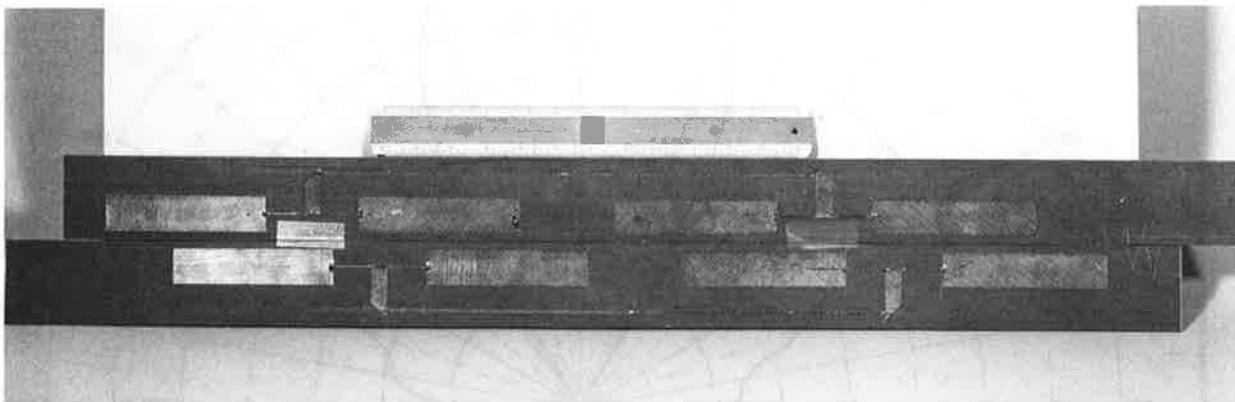
Figure 5-15   End-Fire Array for Switched-Beam Array, Linearly Polarized
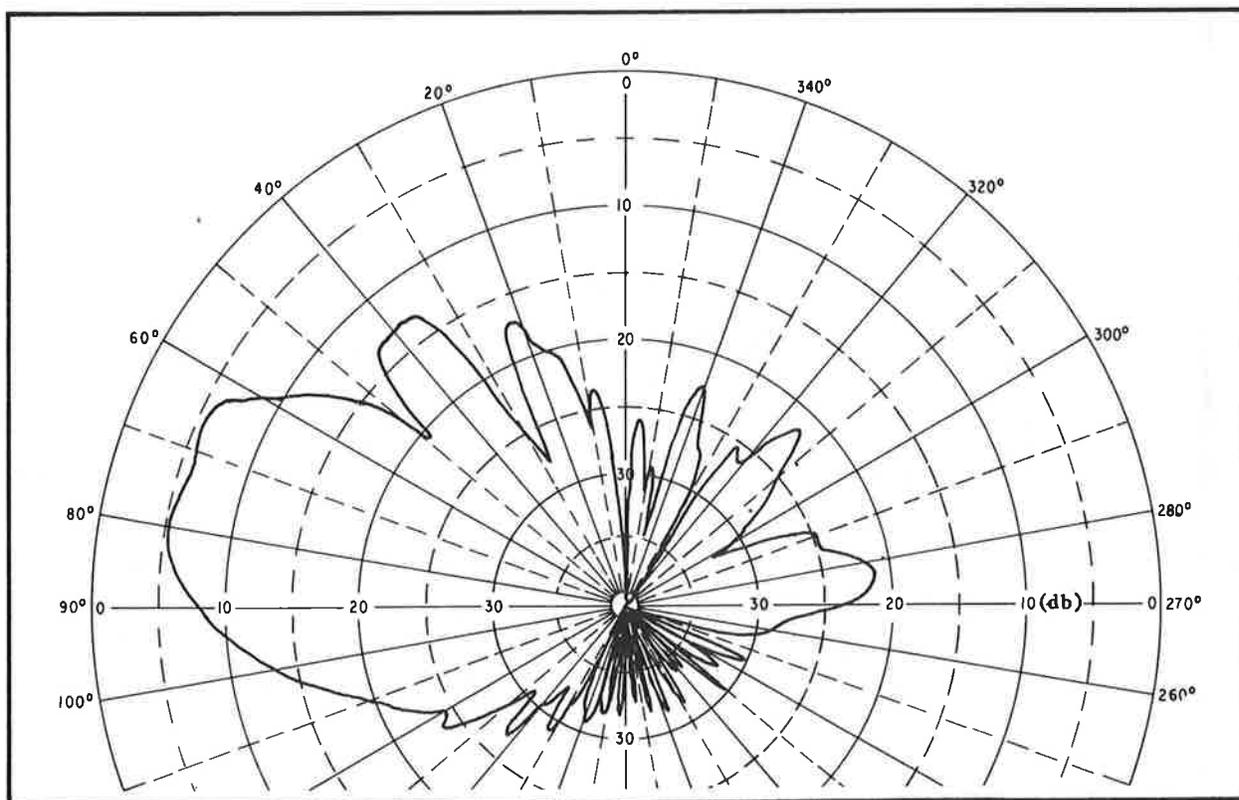
Figure 5-16   Radiation Pattern of Linearly Polarized End-Fire Array

hemispherical array but needs more study before it can be applied to a cylindrical surface.

6.   PHASE-SHIFTER DEVELOPMENT

6.1 PHASE-SHIFTER REQUIREMENTS

The phase-shifter to be used with the phased-array has been developed to meet a range of requirements. A switched-line phase-shifter with series diodes was selected over other designs including a switched-line with shunt diodes and a quadrature-hybrid with shunt diodes. All three were fabricated and tested before making the final selection.

Requirements for the phase-shifter include: operation in two frequency bands (1543-1559 MHz and 1644-1660 MHz), phase resolution of at least 3 bits, power handling capacity of approximately 5 watts C.W. RF power, minimum insertion loss, and compact design to minimize the required installation area on an aircraft.

A requirement for constant phase-versus-frequency response was eliminated when the computer analysis, discussed under Section 5.1 "Phased-Array Analysis," demonstrated that acceptable array performance could be achieved with a linear phase-versus-frequency response. In general, phase-shifters exhibiting a linear phase-versus-frequency response are less complicated and less difficult to implement than others.

6.2 QUADRATURE-HYBRID PHASE SHIFTER

One phase-shifter which exhibits the constant phase-versus-frequency characteristic is a quadrature-hybrid, reflection-type phase shifter, shown in Figure 6-1. This type of phase-shifter is larger than other types in area per bit. Each hybrid is on the order of $\lambda/4$ on a side. Therefore, a 3-bit phase shifter using the quadrature-hybrid would be on the order of $3\lambda/4 \times \lambda/4$ in size. This is too large to be compatible with a conformal microstrip phased-array, especially one in which the close element spacings necessary for end-fire operation are contemplated.

Figure 6-1 Artwork for 180° Quadrature-Hybrid Phase Shifter

An additional problem with this type is the PIN-diode reactance which must be tuned out with a resonant circuit on each of the two coupled ports of the hybrid. At the frequency of interest, the resonant circuit requires a large series inductance to tune to a constant phase slope. This inductance is a problem because of the tiny coils needed to provide it. These coils were not repeatable. The fact that the coils were not identical led to increased insertion loss due to recombination of the out-of-phase reflections in the hybrid.

The advantages of the quadrature-hybrid phase-shifter are that only two diodes are required, and the diodes are conveniently shunt-mounted. Shunt mounting permits better heat sinking and therefore higher power operation than series mounting. For these reasons a quadrature-hybrid phase-shifter was fabricated and tested. Data measured on a 90° and a 180° bit are presented in Figure 6-2. The average maximum insertion loss for the 90° and 180° bits was approximately 0.4 dB and 0.5 dB, respectively, which is typical for this type of phase-shifter circuit. The artwork for the 180° bit is shown in Figure 6.1.

6.3 SWITCHED-LINE PHASE SHIFTER

A switched-line phase-shifter circuit was considered for its simplicity and reduced size. The first design investigated used shunt-mounted PIN diodes because of their increased power handling capability and better heat sinking as compared with series-mounted diodes. This diode also incorporated phase compensation (as described by Burns, et al., see bibliography) to give a constant phase-versus-frequency response. The circuit used three PIN diodes, two in the delay path and one in the reference path. The artwork for this phase-shifter is shown in Figure 6-3.

Both the constant-phase and the linear-phase versions of this phase-shifter exhibited narrow bandwidth and high insertion loss. A better choice of diodes might alleviate this problem. These characteristics are intolerable
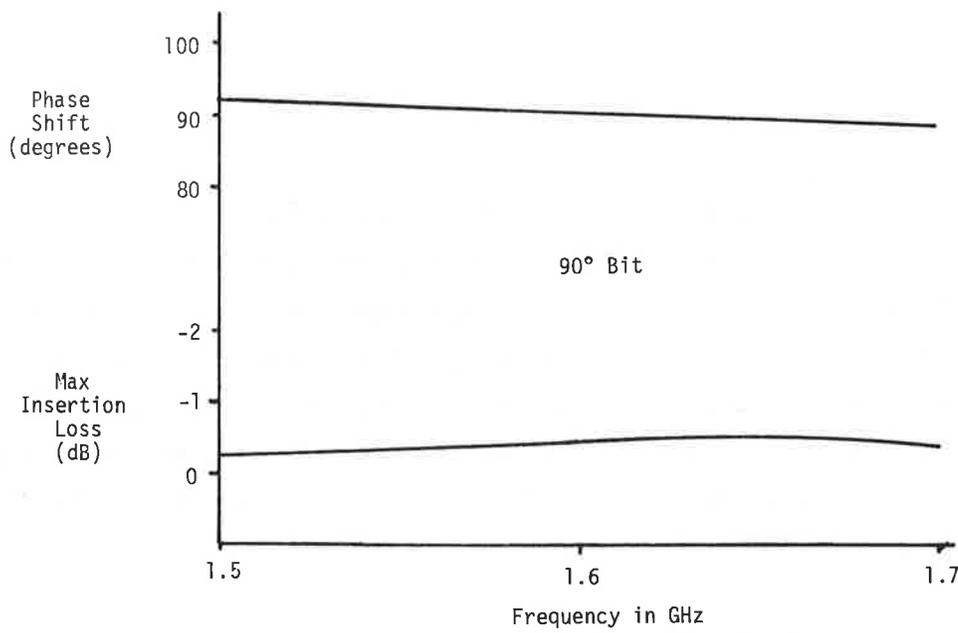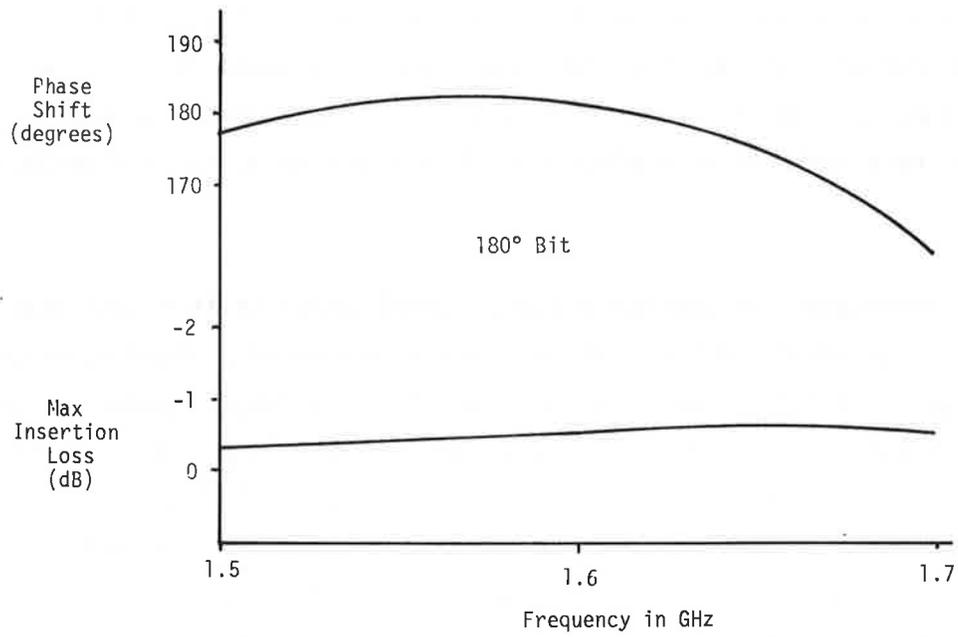
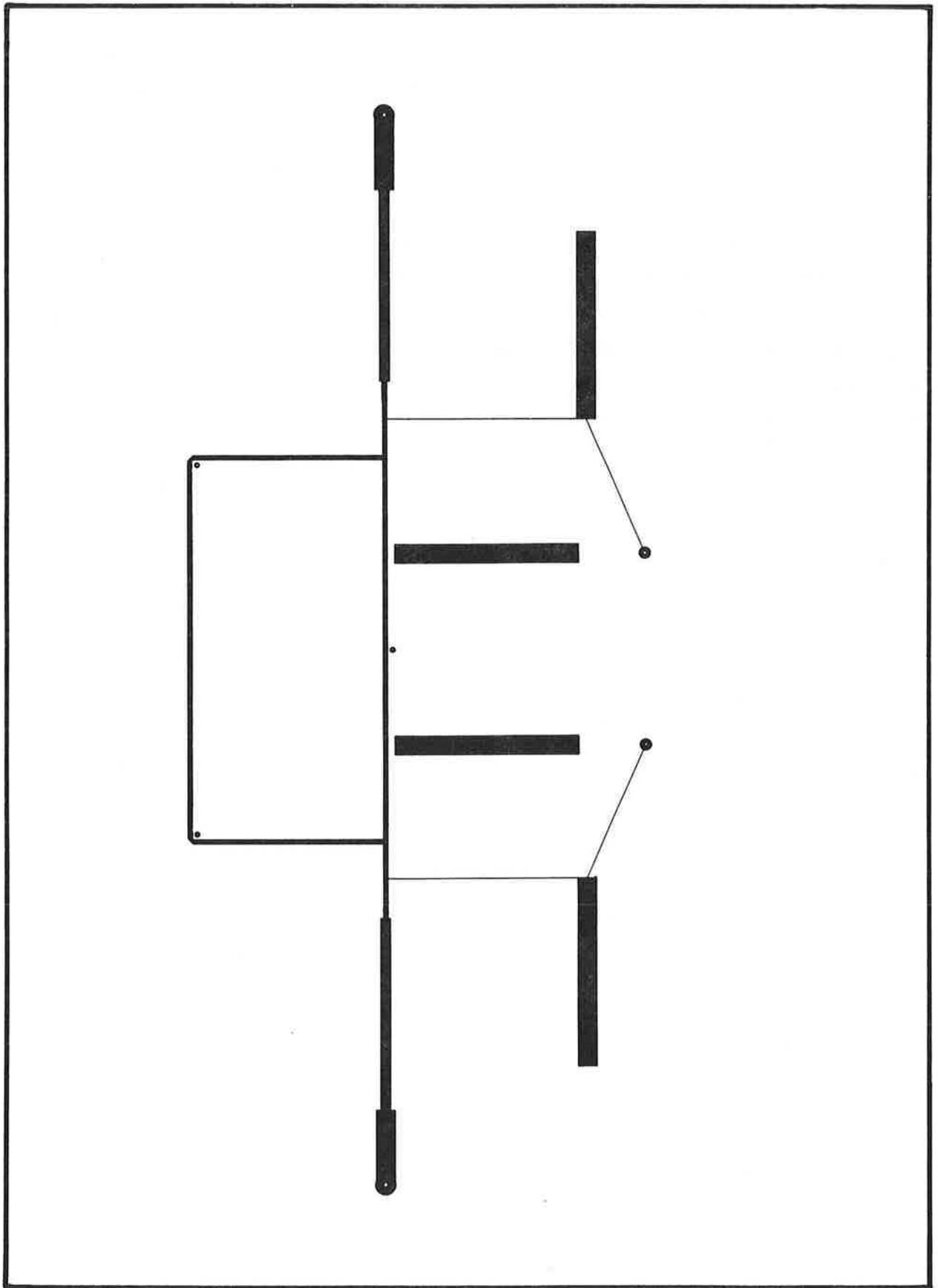Figure 6-2 Quadrature-Hybrid Phase Shifter, Measured Performance

Figure 6-3 Artwork for Single-Bit Switched-Line Phase Shifter with Phase
versus Frequency Compensation

for the present application. Attempts were made to widen the bandwidth of the device but they were not successful. Figure 6-4 shows the phase shift performance with and without the phase-compensating stubs, and Figure 6-5 shows the insertion loss.

In order to achieve lower insertion loss than was measured for the previously mentioned designs, a switched-line phase-shifter using series-mounted diodes was investigated. This phase-shifter is the smallest in area. It does have low insertion loss when the appropriate diode is used on the appropriate line impedance. The circuit can be phase compensated to give a constant phase-versus-frequency response, if necessary. A disadvantage of using this circuit is that it cannot handle high RF power when simply mounted on the surface of the substrate. This is due to the poor heat transfer characteristics of the substrate material. In shunt-mounted designs, the diode is directly connected to the ground plane both electrically and mechanically. This provides excellent heat sinking. However, in low- to medium-power applications, the series-mounted diodes can be used since there is enough thermal conductivity to maintain reasonable junction temperatures. The question of the power handling capacity of series-mounted diodes for this application is discussed further in Section 6.3.

Series-mounted diodes were tested in both 50 ohm and 100 ohm three-bit digital phase-shifters. The insertion loss of the 100 ohm phase shifter was lower than the 50 ohm version, as expected. The insertion loss and isolation of a series-mounted PIN diode is given in Table 6-1. These equations show that by doubling the line impedance the insertion loss per diode is cut in half while the isolation is reduced by 6 dB.
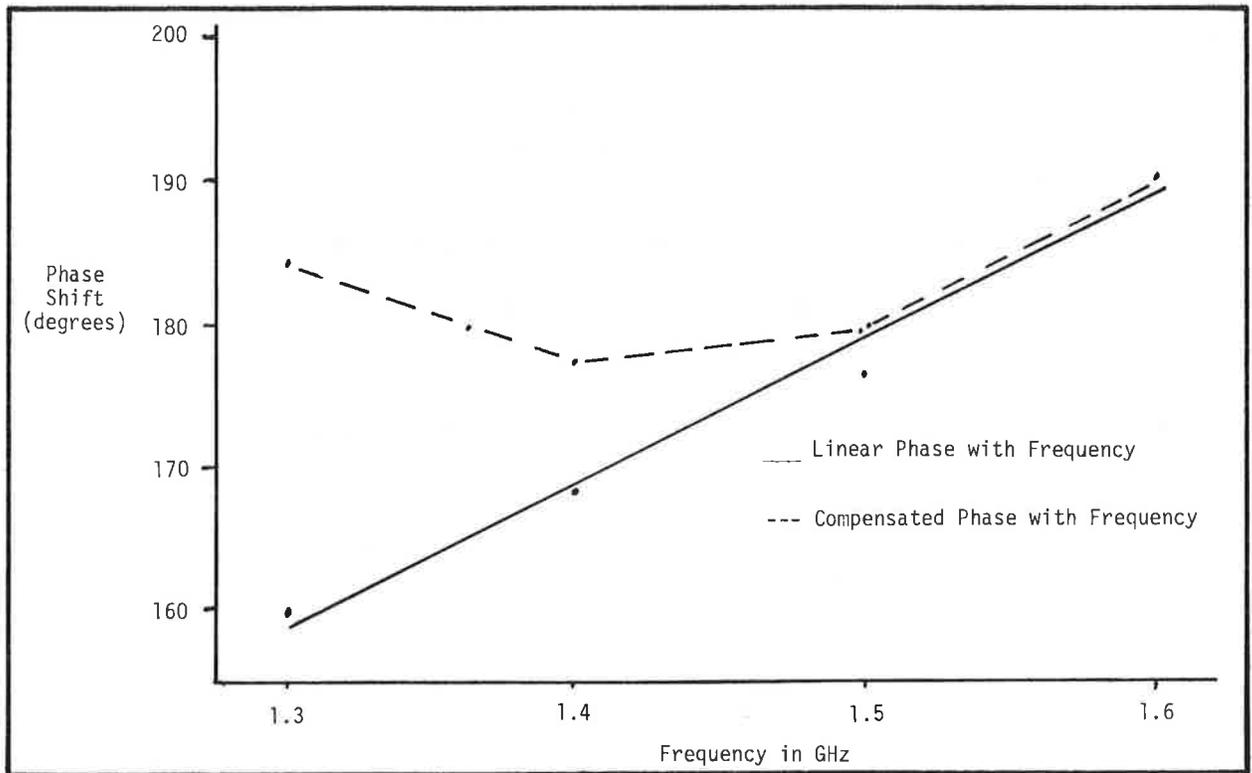
Figure 6-4 Plot of Phase versus Frequency for Switched-Line Phase Shifter
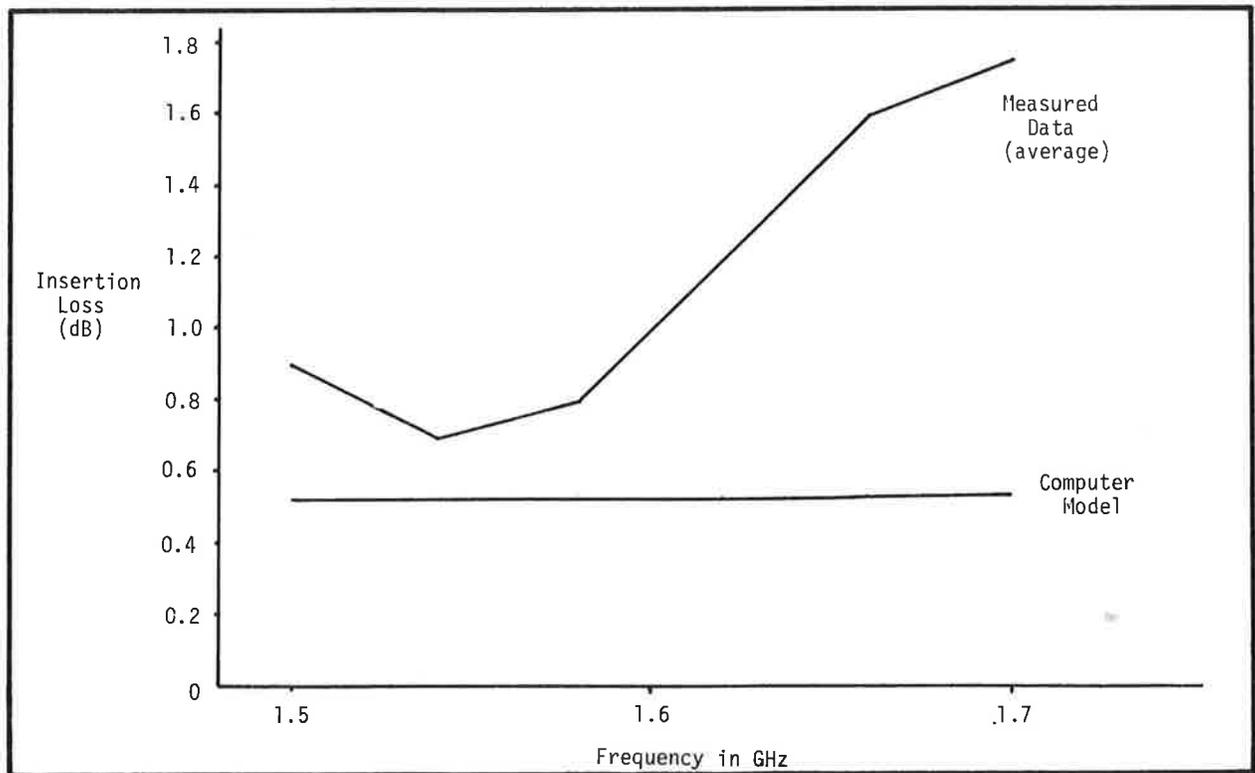
Figure 6-5 Plot of Insertion Loss for Switched-Line Phase Shifter

Table 6-1
SERIES MOUNTED PIN DIODE CHARACTERISTICS
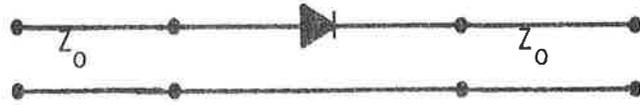
Insertion Loss (dB) = 20 Log $\left[1 + \dfrac{R_s}{2\,Z_0} \right]$

Isolation (dB) = 10 Log $\left[1 + \left(\dfrac{X_c}{2\,Z_0}\right)^2 \right]$

Z_0 = Transmission Line Impedance

R_s = Forward Bias Diode Resistance

$X_c = \dfrac{1}{\omega C}$

C = Reverse Bias Junction Capacitance

$\omega = 2\pi f$

The theoretical insertion loss of the series-mounted diode on a 100 ohm line was .09 dB per diode. The isolation of this diode in reverse bias was 24 dB. Also, on a 100 ohm line the power dissipation of the diode is half of what it would be on a 50 ohm line. This results in lower junction temperatures and better power handling even though the average RF voltage is increased compared to the 50 ohm line.

The artwork for the 100 ohm switched-line, three-bit phase-shifter is shown in Figure 6-6, and Figure 6-7 is a photograph of the working model. Measured insertion loss and phase shift are shown in Figure 6-8. In summary, the data shows a maximum total insertion loss of 1.3 dB and a minimum of

Figure 6-6   Artwork for Switched-Line Three-Bit Phase-Shifter Circuit Using
100 Ohm Transmission Line

Figure 6-7   Photograph of Switched-Line Three-Bit Phase-Shifter Circuit Using
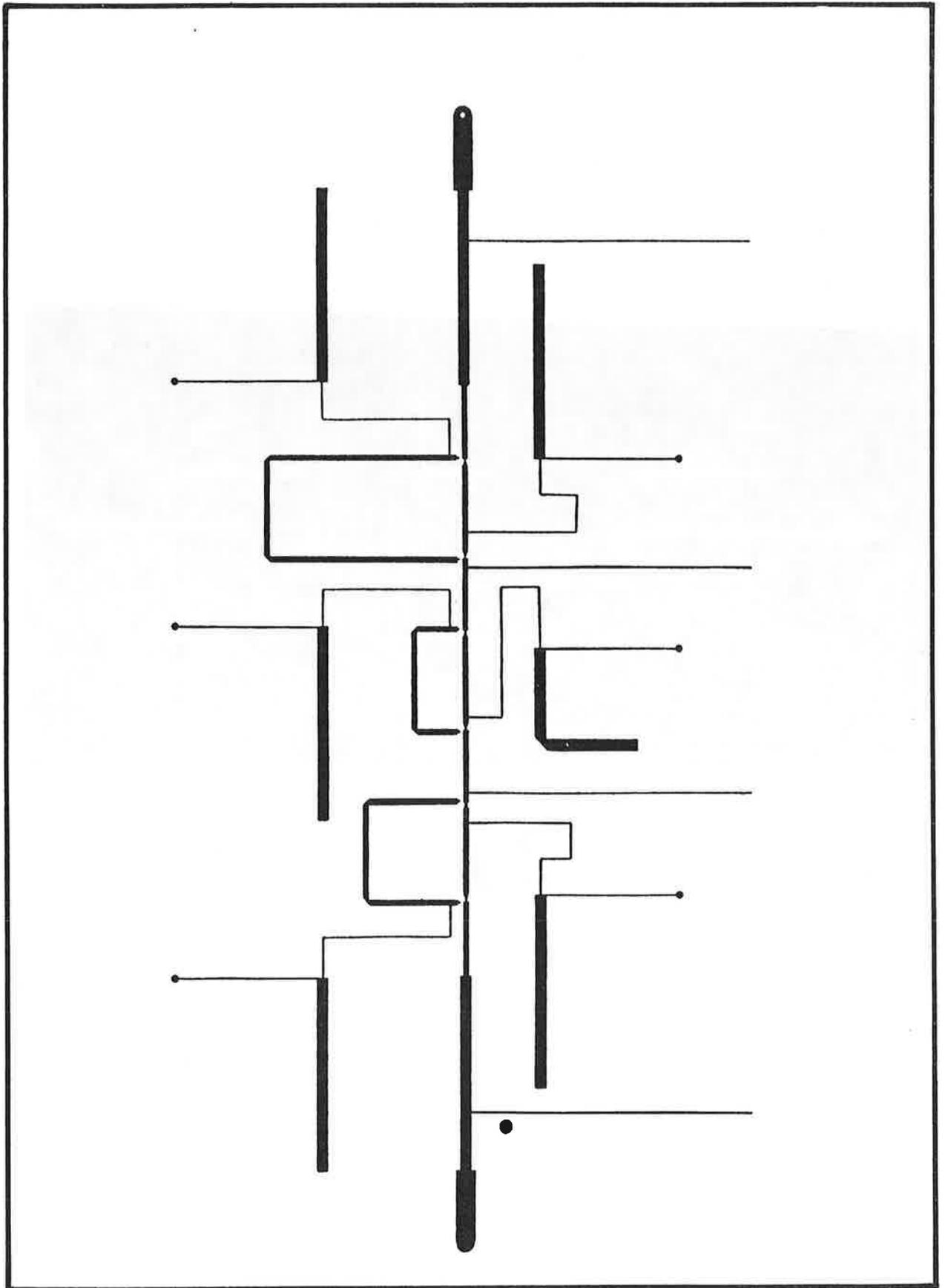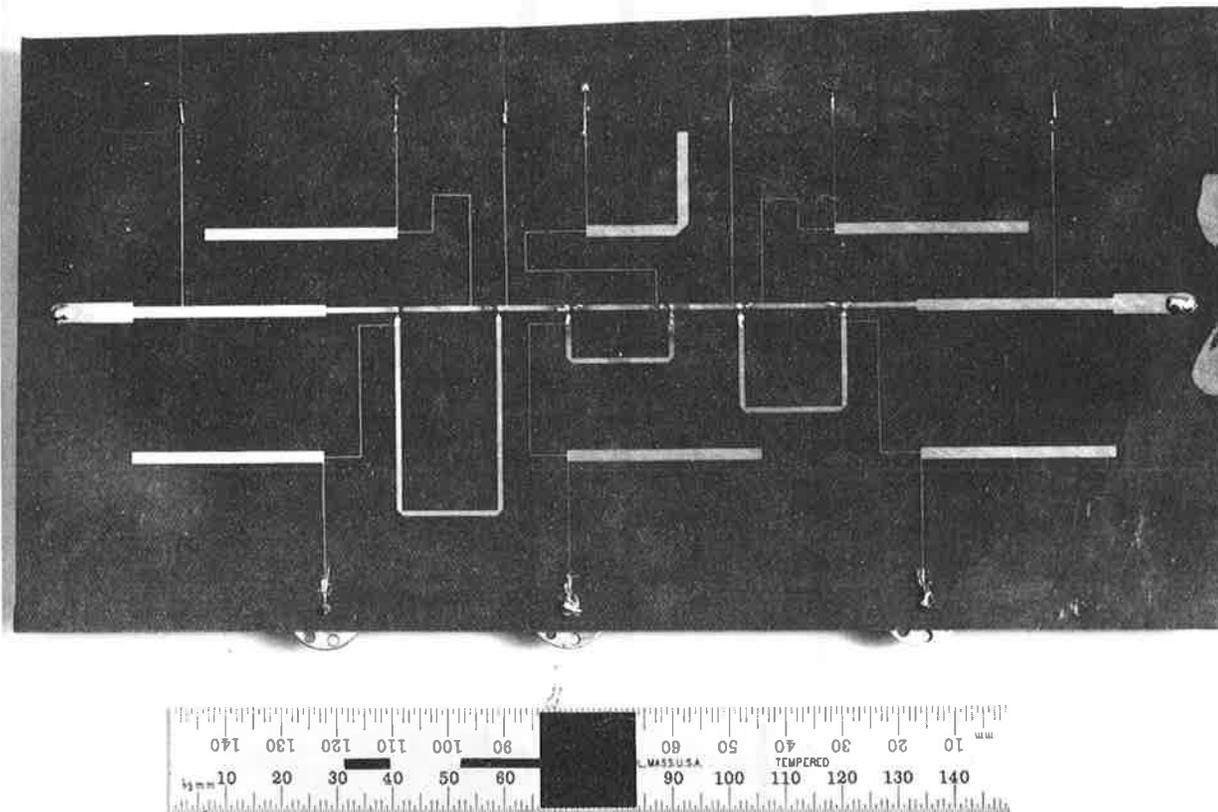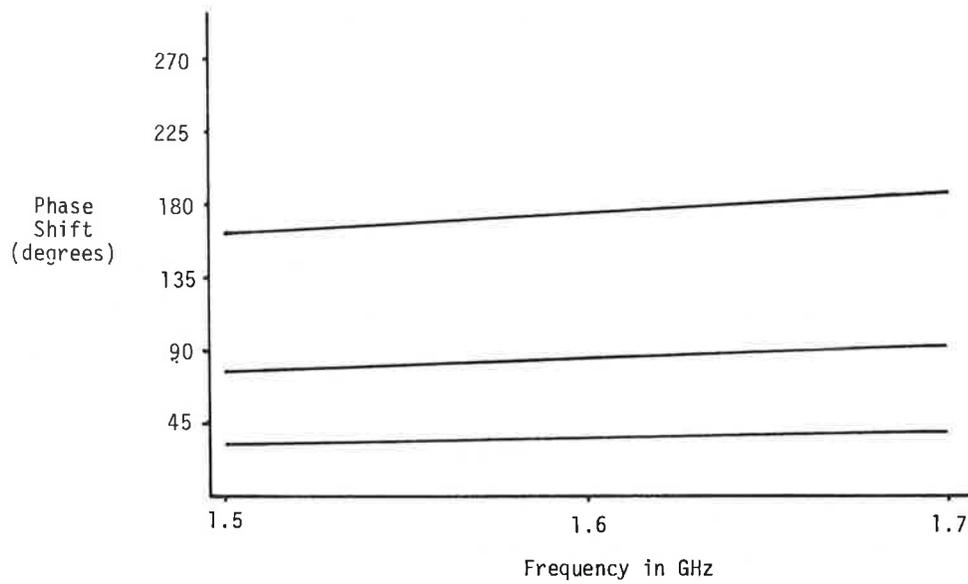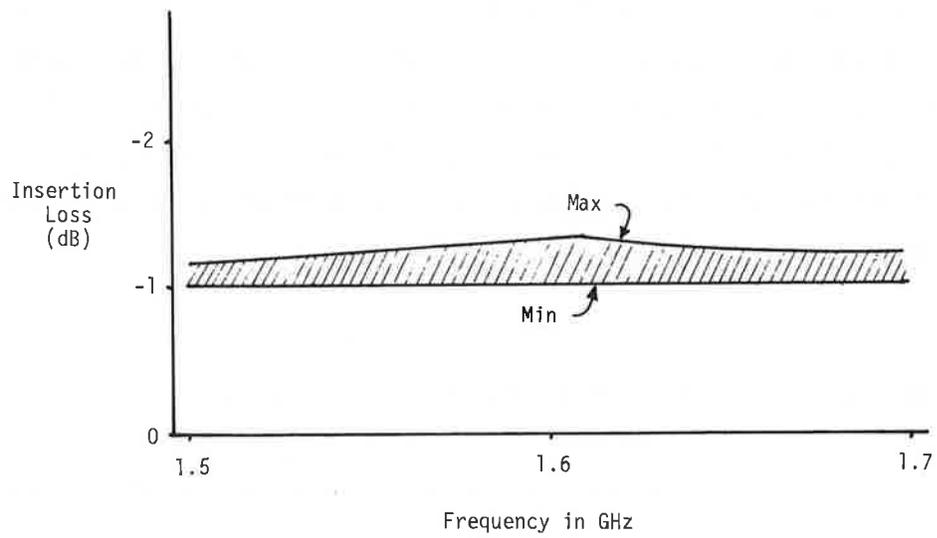100 Ohm Transmission Line

6-10

Figure 6-8 Plot of Insertion Loss and Phase Shift of Switched-Line Three-Bit
Phase Shifter Using 100 Ohm Transmission Line

1.0 dB in the frequency range from 1.5 to 1.7 GHz for all phase states. This loss includes losses due to connectors and matching transformers. These components will not be present in the phased array and can result in a decrease of .2 to .3 dB in the insertion loss. Phase shift is a function of the length of the delay path relative to the reference path. Therefore, it is easily adjusted by varying this length. The measured phase shift of this device was 32°, 80° and 174° for the 45°, 90° and 180° bits, respectively. The measured VSWR for all phase states over the frequency range of 1.5 - 1.7 GHz was less than 1.5:1.

6.4 POWER HANDLING FOR THE SWITCHED-LINE PHASE SHIFTER WITH SERIES DIODES

Series-mounted diodes are not connected to the ground plane and cannot take advantage of that surface as a heat sink. An attempt was made to purchase series diodes mounted on a beryllium oxide pedestal to provide heat sinking to the ground plane without electrically shorting the RF to the ground. This was found to be needlessly expensive and the attempt was abandoned; however, this approach to providing a high-power series design is available, should it be required operationally.

Concurrent with this effort, the phase-shifter described above was analyzed and tested at high power to determine if it could withstand C.W. power levels of up to 7.5 watts. An analysis of PIN diodes on 100 ohm microstrip line was performed. This was based on the thermal impedance of the diode chips mounted on a Duroid substrate. The thermal impedance, Θ, for our specific diode is about 100-150°C/watt. Since the diode has 2 ohms forward series resistance, 2% of the power on a 100-ohm transmission line will be dissipated in the diode. Therefore, if 5 watts C.W. is applied to the circuit, 100 milliwatts will be dissipated in the diode. This will result in a corresponding junction temperature rise given by ΘP_D or (250°C/watt)(.1 watt) for a temperature rise of 25°C. The industry standard for maximum temperature for safe operation is 115°C. Therefore, this limit should not be approached in the present configuration even at ground temperatures of 150°F, and specially mounted diodes should not be required.

The first set of measurements was taken with the phase-shifter at 70°F. Later, the tests were repeated in an oven to raise the temperature of the phase shifter to 150°F. The tests consisted of applying C.W. RF power levels at 1.6 GHZ from 1 watt up to 7.5 watts to the phase-shifter. This was done for 5 of the 8 possible phase states of the 3-bit device. Input power and output power at the device under test were monitored and recorded to give rough insertion loss values at each power level. Table 6-2 shows the data taken for the 70°F case. The average loss for this test for all phase states and for all power levels was 1.21 ± .08 dB. In Table 6-3, the results of the 150°F test are tabulated. The average loss for this test for all phase states and for the power level measured was again 1.21 ± .1dB.

Further tests were run to determine if "hot" switching the diodes would be possible at these power levels. In these tests a switch box employing toggle switches was used to control the phase shifter. Tests showed that the phase-shifter could survive toggle switching the diodes at proven levels up to 5 watts. At 5 watts a diode in the 45° bit was damaged when hot switched. After replacing this diode the test was repeated. Again, a diode in the 45° bit was damaged. It is postulated that the toggle switch on the switch box that was used to control the 45° bit had a greater "bounce" than the other toggle switches. If "hot" switching capability of the phase shifter is necessary, electronic driver circuits should be used to decrease the switching time and reduce the "bounce" effect.

The series-mounted diode configuration was judged to be the most desirable. The series-mounted diode is able to handle power levels below 10 watts without resorting to the use of a beryllium oxide pedestal. It also has the advantage that it uses less area than the shunt-mounted diode configuration.

Table 6-2

INSERTION LOSS OF PHASE SHIFTER AT 70°F

PHASE SETTING (DEGREES)	Power Level Input to Phase Shifter (Watts)				
	.75	2.25	3.75	6	7.5
0	1.14 dB	1.26 dB	1.18 dB	1.28 dB	1.24 dB
45	.98	1.10	1.05	1.14	1.12
90	1.09	1.20	1.13	1.21	1.18
180	1.19	1.28	1.24	1.28	1.29
315	1.09	1.20	1.15	1.21	1.18

Table 6-3

INSERTION LOSS OF PHASE SHIFTER AT 150°F

PHASE SETTING (DEGREES)	Power Level Input to Phase Shifter (Watts)				
	.75	2.25	3.75	6	7.5
0	1.01 dB	1.15 dB	1.16 dB	1.25 dB	1.25 dB
45	1.01	1.08	1.04	1.18	1.19
90	1.07	1.15	1.16	1.25	1.31
180	1.19	1.23	1.27	1.32	1.31
315	1.13	1.15	1.16	1.25	1.25

7. BIBLIOGRAPHY

1. "Air Traffic Control Experimentation and Evaluation with the NASA ATS-6 Satellite," ATS-6 Final Report, Vol. VII, Report No. FAA-RD-75-173-7, April 1976.

2. "Conformal Microstrip Antennas and Microstrip Phased Arrays," Munson, R. E., IEEE Transactions on Antennas and Propagation, Vol. AP-22, No. 1, January 1974, pp. 74-78.

3. "Conformal Microstrip Phased Array for Aircraft Tests with ATS-6," Sanford, G. G., Proceedings of the National Electronics Conference, Vol. XXIX, 1974, pp. 252-257.

4. "Development and Test of a Conformal Microstrip Airborne Phased Array for Use with the ATS-6 Satellite," Sanford, G. G., and L. Klein, IEE Conference Publication No. 128, 1975.

5. "Increasing the Beam Width of a Microstrip Radiating Element," Sanford, G. G., and L. Klein, Proceedings of the IEEE/APS Symposium, Seattle, Washington, June 1979.

6. "Low Cost Design Techniques for Semiconductor Phase Shifters," Burns R. W., R.L. Holden and R. Tang, IEEE Transactions on Microwave Theory and Techniques, Vol. 22, No. 6, June 1974, pp. 675-688.

7. "Phased Array Aircraft Antennas for Satellite Communications," Mailloux, R. J., Microwave Journal, Vol. 20, Oct. 1977, pp. 38-42.

8. "Recent Developments in the Design of Conformal Microstrip Phased Arrays," Sanford, G. G., and L. Klein, International Conference on Maritime and Aeronautical Satellite Communications and Navigation, IEE Conference Publication No. 160, March 1978, pp. 105-108.

9. "Steerable Beam Array Antenna for Use in ATS-6 Test Program," Sanford, G. G., Final Report, Report No. FA-RD-76-86, May 1976.

APPENDIX
REPORT OF NEW TECHNOLOGY

Work performed under this contract has significantly advanced the state. of the art in conformal antenna design. A list of accomplishments would include the following:

- first all-microstrip crossed slot
- unique dual-frequency crossed-slot designs
- use of high dielectric constant to broaden beamwidth
- simplified conformal end-fire array
- adaptation of phase shifter to dual-frequency operation.

Nevertheless, a diligent review of the work has revealed no innovation, discovery, improvement or invention, other than those previously patented.

220 copies